2023-12-01

An Optimization Procedure to Design Nozzle Contours for Hypersonic Wind Tunnels

Omar Antonio Dominguez
University of Texas at El Paso

AN OPTIMIZATION PROCEDURE TO DESIGN NOZZLE CONTOURS FOR

HYPERSONIC WIND TUNNELS

OMAR ANTIONIO DOMINGUEZ

Master's Program in Mechanical Engineering

APPROVED:

_____

Afroza Shirin, Ph.D., Chair

_____

Joel Quintana, Ph.D., co-Chair

_____

Sergio Luna, Ph.D.

_____
Stephen L. Crites, Jr., Ph.D.
Dean of the Graduate School

INVESTIGATION OF OPTIMIZED NOZZLE CONTOURS IN HIGH-SPEED WIND

TUNNELS

by

OMAR ANTONIO DOMINGUEZ, BSME

THESIS

Presented to the Faculty of the Graduate School of

The University of Texas at El Paso

in Partial Fulfillment

of the Requirements

for the Degree of

MASTER OF SCIENCE

Department of Aerospace and Mechanical Engineering

THE UNIVERSITY OF TEXAS AT EL PASO

December 2023

Acknowledgments

I want to express my sincere gratitude to Dr. Afroza Shirin, Assistant Professor in Aerospace and Mechanical Engineering at the University of Texas at El Paso, for her invaluable mentorship that played a pivotal role in guiding both my research and the development of this thesis, Dr. Joel Quintana, Assistant Professor in Aerospace and Mechanical Engineering at the University of Texas at El Paso and Director of Aeronautics and Defense at the Aerospace Center, for providing me with the opportunity to form part and contribute significantly to the Aerospace Center team. I also want to thank Dr. Sergio Luna, Assistant Professor in Industrial, Manufacturing, and Systems Engineering at the University of Texas at El Paso.

A heartfelt thank you goes to my family and Karla Vasquez for their unwavering support, which has been a constant source of encouragement throughout this process.

Abstract

Supersonic wind tunnels allow scientists and researchers to evaluate and analyze the behaviors of objects under real-life conditions when subjected to supersonic speeds. One of the main complexities when building a wind tunnel is the design of the convergent-divergent nozzle that is used to produce high-speed and high-quality flows. To achieve supersonic speeds, this nozzle adopts a specialized approach that incorporates the complexities of flow compressibility. The compressible effect is accurately evaluated using isentropic relations, allowing for precise determination of stagnation pressure and temperature, and static pressure and temperature relevant to the desired Mach number. Isentropic equations used to define these values, as well as the geometry of the nozzle that generates the supersonic behavior are a fundamental part of the overall design of this nozzle. The project focuses solemnly on three Mach numbers: 4.0, 5.0, and 6.0. These contours are determined by implementing the method of characteristics (MoC) assuming that the environment is under steady, axisymmetric, isentropic, and irrotational flow. The design focuses on a 2-dimensional geometry. The MoC is assumed to be used under inviscid conditions, therefore, the use of the boundary layer correction (BLC) is used to generate viscous contours after analyzing and calculating the boundary layer thickness by running Computational Fluid Dynamic (CFD) simulation using Siemens STAR-CCM+ and analyzing the Mach contour at steady state and transient conditions to visualize the flow's behavior. The optimized geometries present an enhanced flow development achieving the designed Mach numbers, although the flow progression is quite unable to perfectly perform near hypersonic speeds due to the difficulties presented at these velocities, the presented Mach numbers are still achieved.

Table of Contents

List of Tables

List of Figures

1. Introduction

Supersonic aerodynamics, characterized by fluid flow at speeds exceeding the local speed of sound, poses unique challenges and opportunities in the realm of aerospace engineering and fluid dynamics. One of the paramount instruments for exploring supersonic flow behaviors is the convergent-divergent (CD) supersonic nozzle present in high-speed wind tunnels. These nozzles serve as conduits for accelerating airflow, often transitioning from subsonic to supersonic speeds (Pope & Goin, 1965).

The study of supersonic nozzle flows at high Mach numbers is of particular significance in advancing aerospace research and technology. This thesis embarks on an investigation of how these CD nozzles are developed and some of the required parameters required to build them. Additionally, it is demonstrated how these nozzles are optimized to achieve a higher quality flow by studying the boundary layer effects specifically present in turbulent flows.

This research centers on the utilization of the method of characteristics (MoC), a powerful computational tool within the realm of fluid dynamics, for the analysis and design of supersonic nozzles. The MoC offers an approach to develop the proper nozzle contour using the appropriate formulations found in compressible flows at high Mach numbers under inviscid conditions. This inviscid solution is the basis for the high-speed flow analysis which posteriorly incorporates viscous conditions to enhance the nozzle's contour.

To optimize the nozzle, the boundary layer correction (BLC) is required. The inclusion of this correction acknowledges the practical realities of viscous effects in supersonic flow and seeks to enhance the performance of the nozzle's contour by addressing boundary layer phenomena. The boundary layer is a fundamental factor in the nozzle's geometry refinement to increase its performance and potentially produce a more accurate flow downstream. Once the

1

thickness is known, the geometry is then optimized to allow the nozzle to develop its flow accurately with the appropriate geometry and achieve the designed Mach number in effect.

This exemplification works with supersonic and hypersonic speeds, conducting an analysis on Mach numbers 4.0, 5.0, and 6.0 by constructing a computational fluid dynamic (CFD) simulation using Siemens STAR-CCM+. The three velocities are employed to conduct simulations with mathematically calculated contours abiding by multiple theories that characterize the flow behavior at these velocities. The CFD simulations offer an analysis of the inviscid and viscous flow behavior. The inviscid solution for each nozzle had viscous conditions applied to observe and measure the boundary layer thickness. This allowed to optimize the contour by applying the BLC and consequently generate the new contour and obtain a better flow.

Moreover, this analysis ultimately presents the steady state and transient behavior of each nozzle. The time discretization of the transient solution is not a relevant factor in this assessment since the main goal of the transient analysis is to determine how the airflow performs throughout the nozzle.

2.   Literature Review

2.1. Convergent-Divergent Nozzle

The CD nozzle is a vital component used in supersonic wind tunnels. This nozzle design involves two distinctive sections as its name indicates and is illustrated in Figure 2.1. The convergent section of the nozzle gradually decreases the cross-sectional area of the flow path, leading to the throat. This narrowing is carefully engineered to achieve a specific critical cross-sectional area at the throat, which is where the flow becomes choked. In a choked flow condition, the airflow is compressed, resulting in a substantial increase in pressure and temperature. This compression is a fundamental element in achieving supersonic speeds, as it prepares the airflow for the subsequent high-speed expansion.
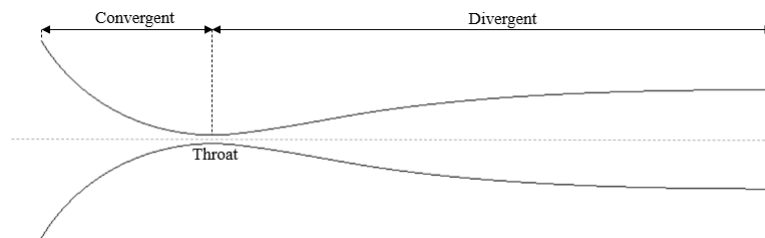
Figure 2.1: Convergent-divergent nozzle schematic

As the airflow passes through the throat and enters the divergent section of the nozzle, the cross-sectional area begins to gradually increase (See section 2.4 for gradual expansion design). This expansion allows the airflow to expand, develop, and accelerate further, while simultaneously reducing pressure and temperature. The gradual expansion of the divergent section enables the flow to reach supersonic or hypersonic velocities, as it is in sync with the increasing speed of the airflow (Deng, 2018).

2.2. Isentropic flow

The nozzle is meticulously designed according to the principles of isentropic flow, which formulate a set of equations used to determine the nozzle's geometry under ideal conditions. Isentropic relations are essential for maintaining a particular thermodynamic state of the airflow.

These relations operate under the crucial assumption that the flow remains isentropic, which implies that the system is both adiabatic (no heat exchange) and reversible (completely recoverable). In the core of the nozzle, the flow exhibits a characteristic of low viscosity, making it akin to an inviscid flow, while near the walls, the substantial viscosity accounts for the boundary layer phenomena due to the no-slip condition (NASA, n.d.).

The inviscid nature of the flow allows us to consider it adiabatic, implying that there is no change in temperature as it moves through the nozzle. Furthermore, the reversibility aspect of the isentropic assumption comes into play, as the gas, once compressed by the nozzle, has the capacity to fully return to its original state without any permanent changes in its physical properties. In essence, the utilization of isentropic flow relations in supersonic nozzle design ensures that the airflow remains in an idealized thermodynamic state throughout its journey, facilitating efficient and controlled supersonic flow within the wind tunnel.

The nozzle's design must respect these isentropic applications, hence, the predefined equations aid in the construction of this geometry. Three equations were used in this setup: equation 2.1 determines the area ratio of the nozzle outlet over the throat. This will provide the aspect ratio between both areas to potentially determine the geometry of the nozzle for the divergent section. Equation 2.2 calculates the static over stagnation pressure (total pressure) ratio, while equation 2.3 obtains the static over stagnation temperature (total temperature) ratio (Pope & Goin, 1965).

$$\frac{A}{A^*} = \left(\frac{\gamma + 1}{2}\right)^{-\frac{\gamma+1}{2(\gamma-1)}} \frac{\left(1 + \frac{\gamma - 1}{2}M^2\right)^{\frac{\gamma+1}{2(\gamma-1)}}}{M} \qquad (2.1)$$

$$\frac{P_S}{P_0} = \left(1 + \frac{\gamma - 1}{2}M^2\right)^{-\frac{\gamma}{\gamma-1}} \qquad (2.2)$$

$$\frac{T_S}{T_0} = \left(1 + \frac{\gamma - 1}{2}M^2\right)^{-1} \qquad (2.3)$$

2.3. The Method of Characteristics

The MoC is a computational technique useful to design supersonic nozzles under two-dimensional, steady, isentropic, and irrotational flows. This technique specifically is applied to design the divergent contour of a supersonic nozzle. The nozzle's convex geometry induces the formation of an expansion fan where flow is "turned away from the main bulk of the flow" (Anderson & Cadou, 2023).

In Figure 2.2, it is observed how this geometry leads to alterations in flow behavior and the corresponding responses of flow properties.
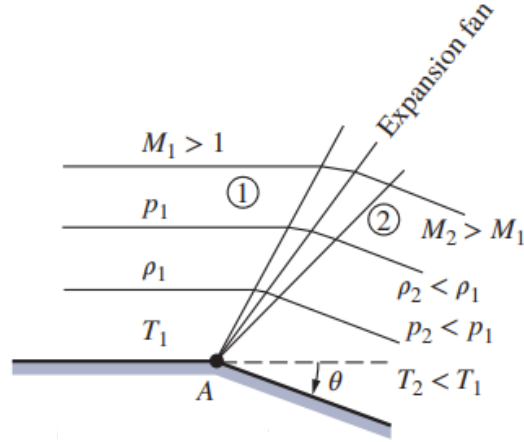
Figure 2.2: Expansion fan (Anderson & Cadou, 2023)

This phenomenon is theoretically identified as the Prandtl-Mayer expansion (v), described by equation 2.4. Here, γ represents the specific heat ratio and M represents the local Mach number.

$$v(M) = \sqrt{\frac{\gamma + 1}{\gamma - 1}} \tan^{-1} \sqrt{\frac{\gamma - 1}{\gamma + 1}(M^2 - 1)} - \tan^{-1} \sqrt{(M^2 - 1)} \qquad (2.4)$$

The change in direction of the flow is to conserve mass. The expansion fan is composed of Mach waves called Prandtl-Mayer expansion waves that are inclined by the local Mach angle (μ) (Cengel & Cimbala, 2017):

$$\mu = \sin^{-1}\left(\frac{1}{M}\right) \qquad (2.5)$$

The MoC creates a flow field by interconnecting a series of grid points, creating a defined mesh. When these grid points are interconnected within a two-dimensional xy space, governed

by a system of partial differential equations, they manifest as what is defined as "characteristic lines" (Anderson & Cadou, 2023).

By implementing the governing equation which encompasses the amalgamation of the continuity, momentum, and energy equations and relating it to the required conditions, it leads to a concise trigonometric definition and reduces the mathematical approach to:

$$\left(\frac{dy}{dx}\right)_{char} = \tan(\theta \mp \mu) \qquad (2.6)$$

The illustration in Figure 2.3 presents a visual representation of equation 2.6, showcasing the interaction of two distinct characteristic lines as they traverse point A. Within this depiction, the streamline exhibits an angle θ relative to the x-axis, while each of the characteristic lines, also referred to as Mach lines, possesses its own unique angle μ. Specifically, C_+ corresponds to the left-running characteristic line, while C_- corresponds to the right-running characteristic line (Anderson, 2020).
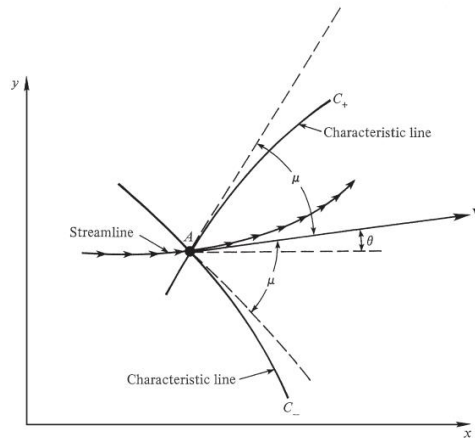

Figure 2.3: Left & right running characteristic lines with respect to streamline (Anderson, 2020)

Subsequently, the next step in the MoC is the derivation of compatibility equations that detail the variation of flow properties along the characteristic lines (equation 2.7). This equation is used for both C_+ and C_- characteristics. By adding the Prandtl-Mayer flow this allows the characteristic lines to relate their velocity magnitude and direction in space. Equations 2.8 and 2.9 are the new derived compatibility equations (Anderson, 2020).

$$d\theta = \mp\sqrt{M^2 - 1}\frac{dV}{V} \tag{2.7}$$

$$\theta + v(M) = K_- \quad (along\ C_-\ characteristic) \tag{2.8}$$

$$\theta - v(M) = K_+ \quad (along\ C_+\ characteristic) \tag{2.9}$$

K_+ and K_- are constants analogous to the Riemann invariants. These new equations are used to determine the grid of the nozzle in two different areas: the internal flow domain and the wall contour.

2.3.1. Internal Flow

When defining each one of the grid points it is assumed that two points are known. There are internal conditions that are already known to create the nozzle. Figure 2.4 illustrates the position of three grid points. The flow properties at point 3 can be directly calculated by knowing the conditions at points 1 and 2 (Vallabh, 2016). Here the values for v_1 and θ_1 are known for point 1, and v_2 and θ_2 are known for point 2. Point 3 is located at the intersection of two characteristics, the C_- characteristic through point 1 and the C_+ characteristic through point 2,

obtaining equations 2.10 and 2.11 which are used to define K_+ and K_- by implementing

equations 2.8 and 2.9.

$$\theta_1 + \nu_1 = (K_-)_1 \tag{2.10}$$

$$\theta_2 - \nu_2 = (K_+)_2 \tag{2.11}$$

Point 3 is obtained by using the C_+ characteristic from point 2 and the C_- characteristic

from point 1:

$$\theta_3 + \nu_3 = (K_-)_3 = (K_-)_1 \tag{2.12}$$

$$\theta_3 - \nu_3 = (K_+)_3 = (K_+)_2 \tag{2.13}$$

By solving equations 2.12 and 2.13. θ_3 and ν_3 are obtained in terms of K_+ and K_- :

$$\theta_3 = \frac{1}{2}[(K_-)_1 + (K_+)_2] \tag{2.14}$$

$$\nu_3 = \frac{1}{2}[(K_-)_1 + (K_+)_2] \tag{2.15}$$

Even though the characteristic lines are showed to be curved, by knowing the location of

points 1 and 2, the accurate solution to locate point 3 is to assume that the characteristic lines are

straight segments between grid points. Figure 2.5 demonstrates that the characteristic lines are

drawn by an average slope angle and their intersection finds point 3 using equations 2.16 and

2.17 (Anderson, 2020).

$$C_+ \, slope = \frac{1}{2}(\theta_1 + \theta_3) - \frac{1}{2}(\mu_1 + \mu_3) \tag{2.16}$$

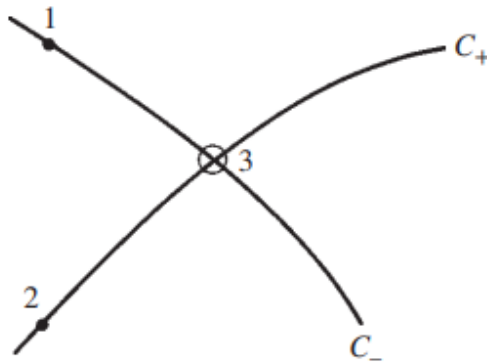$$C_- \, slope = \frac{1}{2}(\theta_2 + \theta_3) - \frac{1}{2}(\mu_2 + \mu_3) \tag{2.17}$$

Figure 2.4: Characteristic mesh used for the location of point 3 and the calculation of

flow conditions at point 3, knowing the locations and flow properties at points 1 and 2 (Anderson
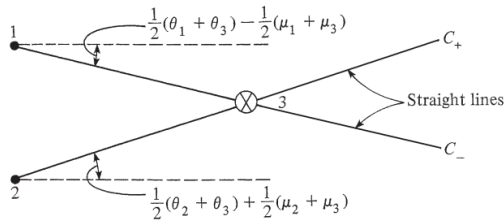
& Cadou, 2023)

Figure 2.5: Approximation of characteristics by straight lines (Anderson & Cadou, 2023).

2.3.2. Wall Points

Figure 2.6 shows the wall contour, and its properties can be determined to obtain the conditions at point 5. Assuming point 4 is known, $(K_-)_4 = \theta_4 + v_4$ is obtained using equation 2.8. The C_- characteristic intersects point 5 at the wall giving equation 2.18:
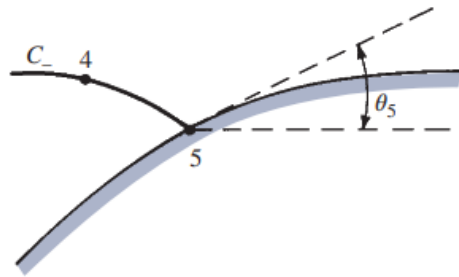
$$(K_-)_4 = (K_-)_5 = \theta_5 + v_5 \tag{2.18}$$

Figure 2.6: Wall point (Anderson & Cadou, 2023)

Since the contour of the nozzle is known, θ_5 is known, leaving v_5 as the only unknown variable, $v_5 = v_4 + \theta_4 - \theta_5$

2.4. Supersonic Nozzle Design

A supersonic nozzle consists of a subsonic and supersonic portion, geometrically denominated by a convergent and divergent region, respectively. The subsonic section accelerates the settling chamber flow delivering a uniform stream through the supersonic section due to the isentropic expansion that occurs due to the change in geometry that starts at the throat.

Improper nozzle contour design can generate unwanted shock waves inside the nozzle. The objective of applying the MoC is to produce shock-free and isentropic flow. (Anderson & Cadou, 2020).

The geometry of supersonic nozzles can vary depending on the application. For rocket nozzle designs where weight is an important factor and proper flow is not important, a minimum-length nozzle is considered. On the other hand, when high-quality flow is required, a gradual expansion nozzle is recommended, often used in high-speed wind tunnels (Khan et al., 2013).

2.4.1. Convergent Section

The convergent section of the nozzle ideally requires a distinct approach to define its geometry. It is composed of an arc with a specified radius that smoothly connects with the curve of the divergent section (Ogawa et al., 2022).

According to Zucrow & Hoffman, Sauers' method for creating the throat curvature profile gives reasonably accurate results and the simplest of many when it comes to two-dimensional nozzles. Figure 2.7 illustrates the general features of the throat having a radius ρ_t. Sauer employs the analysis that the intersection between the sonic line and the x-axis corresponds to the origin of a coordinate system (point 0). The sonic line is a parabola, the locus of all points in the flow fields where the Mach number is 1 (Zucrow & Hoffman, 1977).
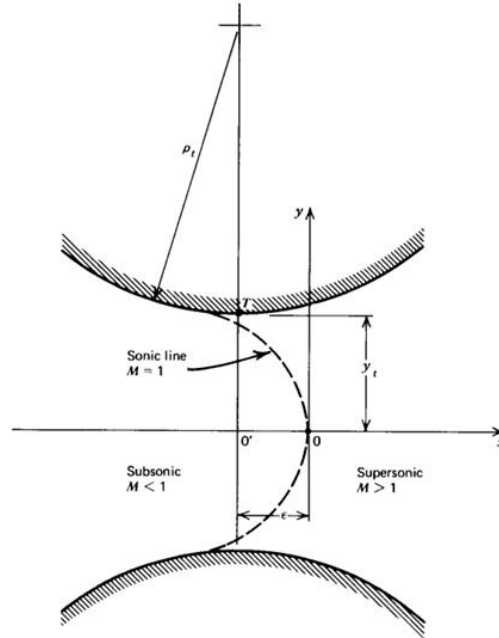
Figure 2.7: Convergent section and throat geometry (Zucrow & Hoffman, 1977)

Some researchers do not generate a convergent section contour with these types of refinements since the focus is mainly sustained in the supersonic section. However, identifying an ideal radius for the curvature between the subsonic and supersonic sections becomes fundamental for optimal flow behavior.

2.4.2. Divergent Section

Utilizing equation 2.1, the parameter A represents the cross-sectional area or height of the nozzle exit. In the case of two-dimensional geometries, the height is used. A^* corresponds to the cross-sectional area or height of the nozzle throat. This ratio is instrumental in delineating the geometric boundaries of the nozzle structure.

Figure 2.8 illustrates the configuration of a supersonic nozzle. After the converging section, the flow undergoes acceleration to attain sonic conditions as it traverses through the throat. This

13

region exhibits a sonic line that is curved. In the context of the MoC, this line is assumed to be straight and is represented by a limiting characteristic (Vallabh, 2016). For gradual expansion nozzles, there are two primary sections that define the contour: the expansion section, and the straightening section. Beyond the throat, the expansion section is characterized by a gradual divergence defined by an increasing wall angle θ_w until reaching a maximum angle θ_{max}, this point is referred to as the inflection point (point 8). Subsequently, it is followed by the straightening section where θ_w starts decreasing until reaching zero or aligns itself parallel to the flow at the nozzle exit. Points 1 and 13 have angles equal to zero. Expansion waves that originate in the expansion section are ultimately canceled in the straightening section (Anderson, 2020).

To effectively cancel an expansion wave, the boundary must satisfy the reflective turning angle of the incoming wave. Hence, the straightening section must exhibit a precise curvature where the incident wave impacts it, with the aim of mitigating wave reflection and rendering the flow parallel to the contour of the nozzle (John & Keith, 2006).

It is important to consider the inflection point or the θ_{max} in the nozzle's design for minimal length and gradual expansion will vary even though they are designed with the same exit Mach number. In the minimum-length nozzle, due to the gradual expansion being replaced by a sharp corner, there are no multiple reflections. On the other hand, the gradual expansion nozzle allows for multiple reflections of the characteristics which allows for a constant acceleration of a fluid element. As a result, θ_{max} in minimum-length nozzle must be larger than in gradual expansion nozzles to satisfy this criterion in terms of equilibrium. Equation 2.19 demonstrates the maximum flow angle for a minimum-length nozzle contour. This is the maximum expansion angle which is equal to one-half of the Prandtl-Mayer function of the design exit Mach number (Anderson, 2020).

$$\theta_{max,\ M_L} = \frac{v(M)}{2} \tag{2.19}$$

In other cases where the expansion angle is arbitrary, this expansion angle is less than $\frac{v(M)}{2}$. As described in the convergent section, the gradual expansion contour is considered as an arc. Once the shape and expansion angle are determined, the characteristic line from the end of the expansion section intersects the centerline further downstream where the local Mach number resembles that of the design Mach number, the contour can be defined (Anderson, 2020).

To achieve higher precision and fidelity in modeling and optimizing gradual expansion nozzles, a more refined computational approach is imperative, one that fully leverages the principles of the method of characteristics.

Due to the increased level of calculations required for the MoC, the nozzle's symmetric geometry can minimize calculations by using the section above the centerline, this practice is frequently considered since the waves produced in the upward section symmetrically reflect in the bottom section (Vallabh, 2016).
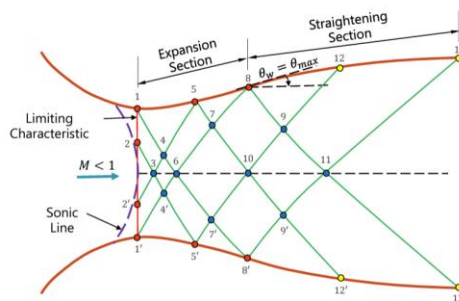
Figure 2.8: Supersonic nozzle schematic using the method of characteristics (MoC)

(Ansys Innovation Courses, 2020)

15

Anderson and Cadou give a great explanation on how to implement this method. Their explanation briefly described how to solve a coarse mesh such as the one seen in Figure 2.8 and can be used as reference to produce a refined grid:

1. Draw a C_- characteristic from point 2, intersecting the centerline at point 3. Evaluating Equation (2.18) at point 3, we have:

$$\theta_3 + v_3 = (K_-)_3$$

   In the above equation, $\theta_3 = 0$ (the flow is horizontal along the centerline). Also, $(K_-)_3$ is known because $(K_-)_3 = (K_-)_2$. Hence, the above equation can be solved for v_3.

2. Point 4 is located by the intersection of the C_- characteristic from point 1 and the C_+ characteristic from point 3. In turn, the flow properties at the internal point 4 are determined as discussed in section 2.3.1.

3. Point 5 is located by the intersection of the C_+ characteristic from point 4 with the wall. Since θ_5 is known, the flow properties at point 5 are determined as discussed in section 2.3.2 for wall points.

4. Points 6 through 11 are located in a manner similar to the above, and the flow properties at these points are determined as discussed before, using the internal point or wall point method as appropriate.

5. Point 12 is a wall point on the straightening section of the contour. The purpose of the straightening section is to cancel the expansion waves generated by the expansion section. Hence, there are no waves which are reflected from the straightening section. In turn, no right-running waves cross the characteristic line between points 9 and 12. As a result, the characteristic line between points 9 and 12 is a straight line, along which θ is

16

constant, that is, $\theta_{12} = \theta_9$. The section of the wall contour between points 8 and 12 is approximated by a straight line with an average slope of $\frac{1}{2}(\theta_8 + \theta_{12})$.

6. Along the centerline, the Mach number continuously increases. Let us assume that at point 11, the design exit Mach number M_e is reached. The characteristic line from points 11 to 13 is the last line of the calculation. Again, $\theta_{13} = \theta_{11}$, the contour from point 12 to point 13 is approximated by a straight-line segment with an average slope of $\frac{1}{2}(\theta_{12} + \theta_{13})$.

2.5. Boundary Layer Correction

"The boundary layer is the thin region of flow adjacent to a surface, where the flow is retarded by the influence of friction between a solid surface and the fluid" (Anderson & Cadou, 2023).

It is important to consider both inviscid and viscous regimes when analyzing the flow in the nozzle. These two terms rely on the definition of a fluid's viscosity. Viscosity is the measure of a fluid's resistance to flow (Princeton, n.d.).

Inviscid flow is when a fluid's viscous effects are neglected, it is assumed to have zero viscosity. Viscous flow refers to a fluid with viscosity, this type of flow generates the boundary layer phenomena due to the no-slip condition. As a result of the viscous effects, temperature rises in the boundary layer due to the friction described earlier in this section.

This boundary layer plays an important role in the creation of the CD nozzle. With the MoC, the contour is created under inviscid conditions, and no viscous properties are considered. When the nozzle contour is developed and analyzed, then the implementation of turbulent viscous flow conditions can be applied. The area ratio from the isentropic equations generates the geometry

for the inviscid solution. To translate it to the viscous solution the BLC is required to optimize the nozzle by fixing its contour with respect to the boundary layer thickness produced at the specified design Mach number.

In a supersonic CD nozzle, the boundary layer is just a fraction of the distance from the wall to the nozzle's centerline. The nozzle wall has a velocity of zero and at the other end of the boundary layer, the velocity is equal to that of the freestream. The boundary layer displacement thickness is often referred as δ^* and can be defined by using the following equation:

$$\delta^* = \int_0^\delta \left(1 - \frac{\rho U}{\rho_e U_e}\right) dy \tag{2.20}$$

Where ρ is the density, U is the free stream velocity, y is the distance from the wall, and δ is the boundary layer thickness (Pope & Goin, 1965). Figure 2.9 depicts how the BLC should correct the nozzle contour.
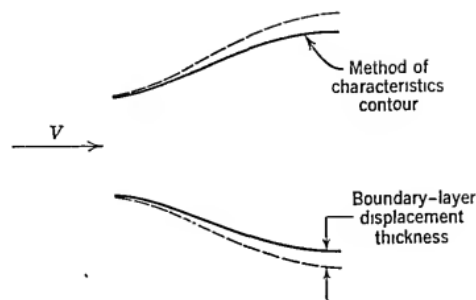
Figure 2.9: Boundary layer correction (BLC) interpretation (Pope & Goin, 1965)

3. Nozzle Structure Development

Planar nozzles (two-dimensional) were the premise in supersonic and hypersonic aerodynamics until inaccuracies due to dimensional stability arose. The introduction of an axisymmetric nozzle became primordial to produce optimized stability in nozzle design. The only drawback is that axisymmetric nozzles can only be designed for a particular Mach number. The development of axisymmetric nozzles can be adapted to planar nozzles by having a prescribed centerline distribution of the Mach number where an analytical solution can be determined by incorporating the MoC given as an optional approach (Sivells, 1978).

Given that axisymmetric nozzles can be constructed based on only half of the entire geometry makes the computational process faster.

The convergent section is implemented by a simple radius intersecting the throat at point 0 as illustrated in Figure 2.7. The designated radius for all three nozzles is set at $100.0\ in$.

For the divergent section, the method of characteristics is employed, and relevant conditions are established. Initially, the area ratio between the throat and the outlet is determined using Equation 2.1. Given the axisymmetric nature of this design, the ratio is derived solely based on heights (y-values) rather than the entire cross-sectional area. The nozzle outlet is positioned $25.0\ in$ above the centerline and $271.33\ in$ from point 0. By employing equation 2.1, the throat height is calculated:

- Mach 4.0 area ratio

$$\frac{A}{A^*} = 10.7188 \qquad \longrightarrow \qquad A = 25.0\ in\ ,A^* = 2.33\ in$$

- Mach 5.0 area ratio

$$\frac{A}{A^*} = 25 \qquad \longrightarrow \qquad A = 25.0\ in\ , A^* = 1.0\ in$$

- Mach 6.0 area ratio

$$\frac{A}{A^*} = 51.1798 \qquad \longrightarrow \qquad A = 25.0\ in\ , A^* = 0.49\ in$$

Another important factor described by Anderson is the maximum expansion angle in the nozzle's contour. In gradual expansion nozzles this value is not directly set by equation 2.19, but it must be lower. Table 3.1 describes the maximum angles used for each contour.

Table 3.1: Expansion angles

Mach Number	Designated $\theta_{max,\ M_L}$ (deg)	Assigned $\theta_{max,\ M_L}$ (deg)
4.0	66.78	10.70
5.0	76.92	10.64
6.0	84.95	13.21
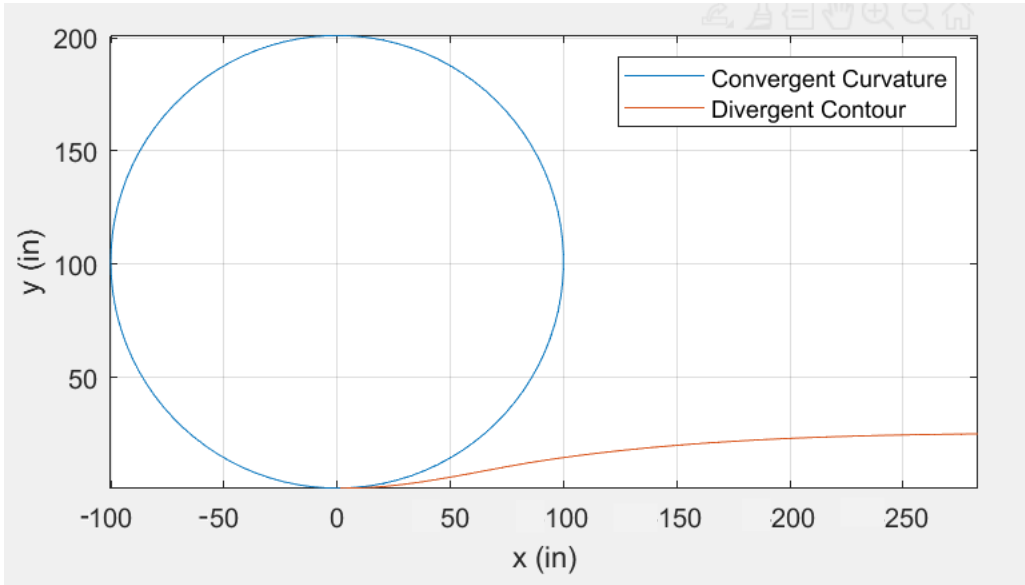
Figure 3.1: Convergent curvature and divergent contour visualization

Only part of the bottom left quadrant of the circle in Figure 3.1 is used to be part of the contour as seen in Figure 3.2.
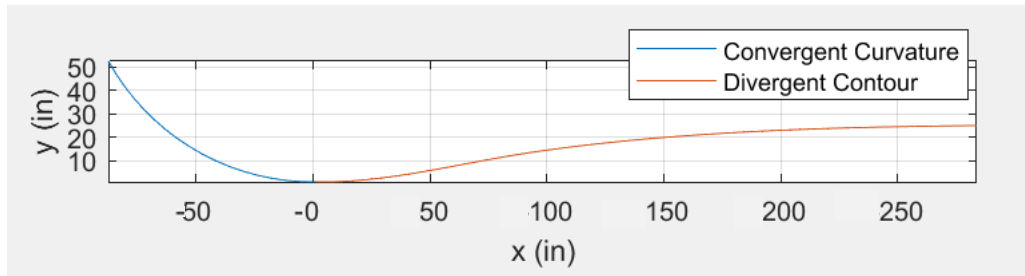
Figure 3.2: Complete inviscid nozzle contour

4.   Computational Fluid Dynamic Setup

All simulations were performed in Siemens STAR-CCM+. The geometry for the Mach 4, 5, and 6 nozzles were obtained using the MoC, importing the coordinates in a comma-separated-values (.csv) file.

For a comprehensive review of how the STAR-CCM+ interface was set up for this analysis, see Appendix.

4.1.   Boundary Conditions

Four different boundary conditions are applied into the nozzle's geometry: inlet, outlet, walls, and a since this is a 2-dimensional solution a symmetry plane is required to generate the 2D mesh. Figure 4.1 illustrates this setup. This setup is equal for all three nozzles.
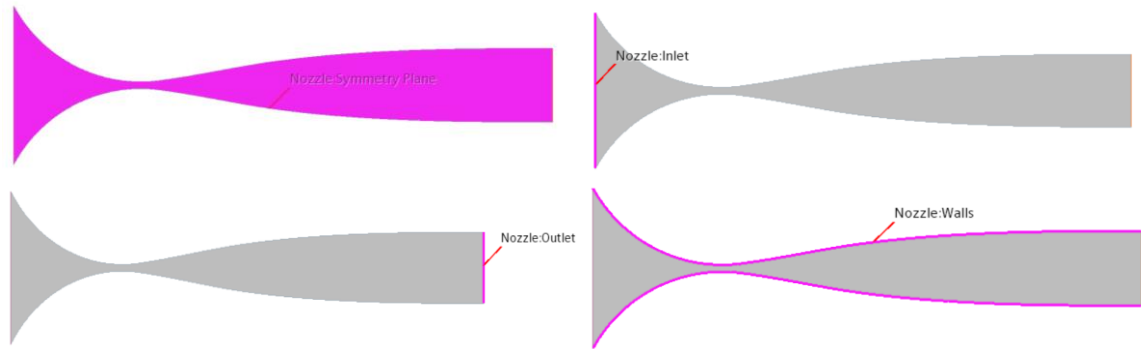
Figure 4.1: Boundary conditions

4.2.   Mesh

Only two meshers were used: polygonal mesher for the mesh cells geometry and prism layer mesher for refinement in the boundary layer sections. Tables 4.1 and 4.2 indicate the values considered and configured to generate the mesh.

Table 4.1: Polygonal mesher parameters.

Polygonal Mesher	
Base Size	1.0 in
Surface Proximity (# of points in gap)	5.0
Surface Growth Rate	Slow

Table 4.2: Prism layer mesher parameters

Prism Layer Mesher	
Number of Prism Layers	10.0
Prism Layer Stretching	1.3
Prism Layer Thickness	4.0 in

The prism layer thickness was set to 4.0 in initially to conduct the viscous analysis with the inviscid contour. This unrelated value helps refine a portion of the near-wall sections to read appropriate dimensions and facilitate prism layer thickness input with each respective nozzle. These dimensions are later discussed. The executed mesh is illustrated in Figure 4.2. The mesh in each nozzle has almost the same number of cells, faces, and vertices approximating to 13,000, 32,000, and 19,000, respectively.
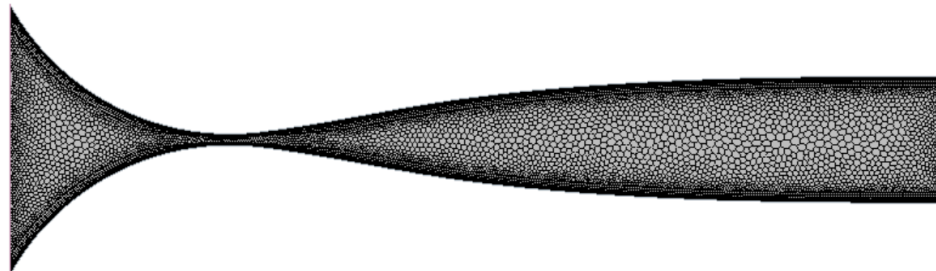
Figure 4.2: Nozzle mesh

4.3. Physics Continua

4.3.1. Models

Air is the only material used in the continuum and some respective parameters are reconfigured to satisfy the system's requirements. The following models were selected to create the nozzle's continuum:

- Space: Two-dimensional

- Time: Steady (Steady-State) and Implicit Unsteady (Transient)

- Material: Gas

  - Air. The dynamic viscosity was set by implementing Sutherlands law which defines the system's viscosity of the gas which is dependent on the local temperature.

- Flow: Coupled Flow

  - This model yields more robust and accurate solutions in compressible flow, especially when shocks are involved. It has better conditioning for supersonic flows by solving the governing equations simultaneously and better capturing the interactions in between. Along with this model, an optional scheme for evaluating inviscid fluxes is Liou's AUSM+ flux-vector splitting scheme. It is appropriate for solving flows involving supersonic regimes. It comes with several advantages that aid the simulation's process: algorithmic simplicity and straightforward extension for complex conservation laws, accurate capture of shock and contact discontinuity, numerical solutions that preserve positivity and satisfy entropy, and reduced susceptibility to "carbuncle" phenomena (Siemens, 2021).

- Equation of State: Ideal Gas

- Viscous Regime: Inviscid and Turbulent

- Reynolds-Averaged Turbulence: K-Epsilon

4.3.2. Initial Conditions

The system requires some initial data to start running the simulation. All nozzles were initialized by setting the initial conditions to Mach 0.8 for steady state. This allows the system to gradually converge the system into reaching steady state. Starting from the desired Mach number might cause instabilities and potentially produce an incorrect solution. These conditions can also be obtained by using the isentropic equations:

$$\frac{P_S}{P_0} = 0.6560 \qquad \longrightarrow \qquad P_S = 12.97\ psi\ , P_0 = 19.50\ psi$$

$$\frac{T_S}{T_0} = 0.8865 \qquad \longrightarrow \qquad T_S = 483.14\ R\ , T_0 = 545\ R$$

The initial conditions were set as seen in Table 4.3.

Table 4.3: Steady state initial conditions

Condition	Value
Pressure	$12.97\ psi$
Static Temperature	$483.14\ R$
Velocity	$[274.4,0]\ {}^{m}/_{s}$

For the transient analyses, the initial conditions are configured to simulate ambient conditions, starting with no velocity. The time-variant discretization facilitates the simulation to progress from ambient conditions, gradually increase the speed as if the nozzle were initiating startup from a state of rest. Table 4.4 demonstrates these values.

Table 4.4: Transient initial conditions

Condition	Value
Pressure	$14.70 \, psi$
Static Temperature	$540 \, R$
Velocity	$[0,0] \, m/s$

4.3.3. Reference Values

The system's input parameters are a fundamental part of the simulation. It is important to specify the range onto which the solution will be solved. Based on several simulations performed, it is optimal to use the values obtained in section 4.5 as the reference values in the system. Tables 4.5 – 4.7 depict this setup for each Mach number.

Table 4.5: Mach 4.0 reference values

Mach 4.0	
Parameter	Value
Reference Pressure	$0 \, psi$
Minimum Allowable Absolute Pressure	$1.91 \, psi$
Minimum Allowable Temperature	$129.76 \, R$
Maximum Allowable Absolute Pressure	$290 \, psi$
Maximum Allowable Temperature	$545 \, R$

Table 4.6: Mach 5.0 reference values

Mach 5.0	
Parameter	Value
Reference Pressure	$0\,psi$
Minimum Allowable Absolute Pressure	$0.56\,psi$
Minimum Allowable Temperature	$90.83\,R$
Maximum Allowable Absolute Pressure	$310\,psi$
Maximum Allowable Temperature	$545\,R$

Table 4.7: Mach 6.0 reference values

Mach 6.0	
Parameter	Value
Reference Pressure	$0\,psi$
Minimum Allowable Absolute Pressure	$0.22\,psi$
Minimum Allowable Temperature	$66.49\,R$
Maximum Allowable Absolute Pressure	$350\,psi$
Maximum Allowable Temperature	$545\,R$

All values obtained by the isentropic equations are absolute, hence the $0\,psi$ value for the reference pressure.

4.4. Solvers

For the steady state solver, only the Courant-Friedrichs Lewy (CFL) stability condition is applied. To reach a stable solution this value must be low; it ensures that the numerical solution remains accurate by restricting the size of time steps based on the system's properties and grid spacing. This value is set to solve within an automated range, but it has been configured for it to have an initial value of 1.0 and a maximum value of 10.0.

The transient solution also requires the same configuration for the CFL number plus the explicit relaxation, which is automatically set to 0.3 when activated, this value will be used for the transient simulations.

Explicit relaxation is a scaling factor that is used to relax all coupled flow corrections explicitly before they are applied to the flow solution, also known as a damped update. This generally improves numerical stability and convergence, particularly when running at a high CFL number. For the unsteady solver, the default is None, as time-accurate integration usually provides sufficient stability (Siemens, 2021). Although Siemens specifies that this method is not a default parameter due to its apparent unrequired use, the solution present necessitates this input for optimal convergence. The consequence of using this in implicit unsteady solutions is that it becomes time-consuming.

4.5. Regions

All three nozzles have the same boundary conditions but require further assessment. A boundary type must be assigned to input the necessary values for pressures and temperatures. Table 4.7 specifies the boundary types described in Siemens STAR-CCM+ manual.

Table 4.8: Boundary types

Boundary Condition	STAR-CCM+ Boundary Type	Description
Inlet	Stagnation Inlet	The stagnation conditions refer to the conditions in an imaginary plenum, far upstream, in which the flow is completely at rest.
Outlet	Pressure Outlet	Outlet boundary at which the pressure is specified.

Wall	Wall	Represents an impermeable surface
Symmetry	Symmetry Plane	Represents an imaginary plane of symmetry in the simulation.

Each nozzle has a set of specific values which are obtained by using the isentropic equations (Equations 2.2 & 2.3). The specific heat ratio $\gamma = 1.4$ for air. M equals the design Mach number. The stagnation and static values must be adequate to the simulation and tests are necessary to see if they work. Not because they satisfy the ratio from the isentropic equations means that it's the ideal value to use. The following values were evaluated before analyzing results to meet the design Mach number in the results.

- Mach 4.0 pressure and temperature values

$$\frac{P_S}{P_0} = 0.0066 \qquad \longrightarrow \qquad P_S = 290.0 \ psi \ , P_0 = 1.91 \ psi$$

$$\frac{T_S}{T_0} = 0.2381 \qquad \longrightarrow \qquad T_S = 129.76 \ R \ , T_0 = 545 \ R$$

- Mach 5.0 pressure and temperature values

$$\frac{P_S}{P_0} = 0.0019 \qquad \longrightarrow \qquad P_S = 310.0 \ psi \ , P_0 = 0.59 \ psi$$

$$\frac{T_S}{T_0} = 0.1667 \qquad \longrightarrow \qquad T_S = 90.85\ R\ , T_0 = 545.0\ R$$

- Mach 6.0 pressure and temperature values

$$\frac{P_S}{P_0} = 0.0006 \qquad \longrightarrow \qquad P_S = 350.0\ psi\ , P_0 = 0.22\ psi$$

$$\frac{T_S}{T_0} = 0.1220 \qquad \longrightarrow \qquad T_S = 66.49\ R\ , T_0 = 545.0\ R$$

5. Results

Numerous design interations were developed to produce the optimized contours, ensuring the desired velocity and proper airflow were observed. A systematic process was adopted to implement corrections and ascertain the optimal design for meeting the specified requirements. Figure 5.1 shows a flow chart that encapsulates this design process.
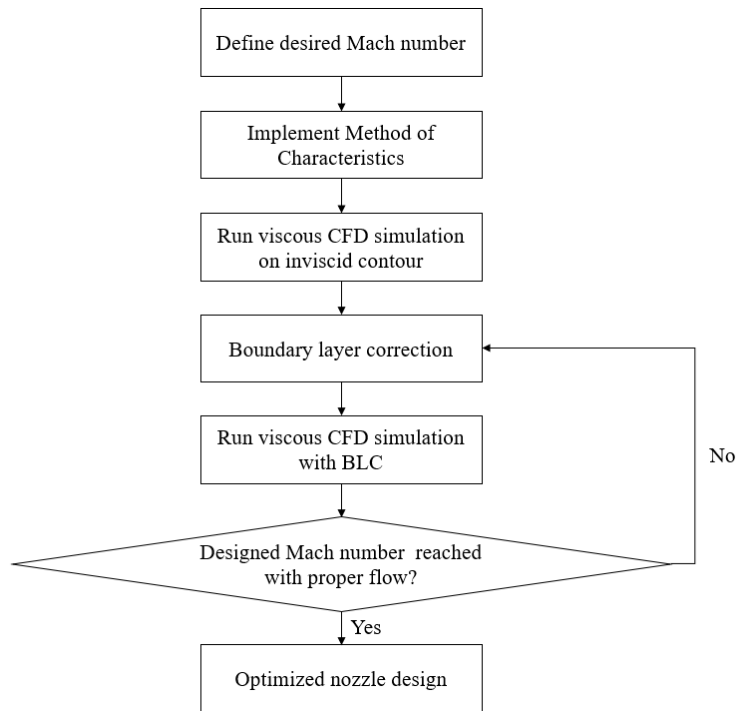
Figure 5.1: Nozzle design process

5.1. Inviscid Contour Analysis

Having the contours defined for each Mach number and abiding by the applying principles, the CFD simulations are used to capture the flow profile in each nozzle and observe the behavior when applying these parameters. Each simulation conducted was configured to achieve 2000 iterations to reach convergence in a viscous state so that the boundary layer could develop properly to then implement the BLC and adjust the contour accordingly.

- Mach 4.0
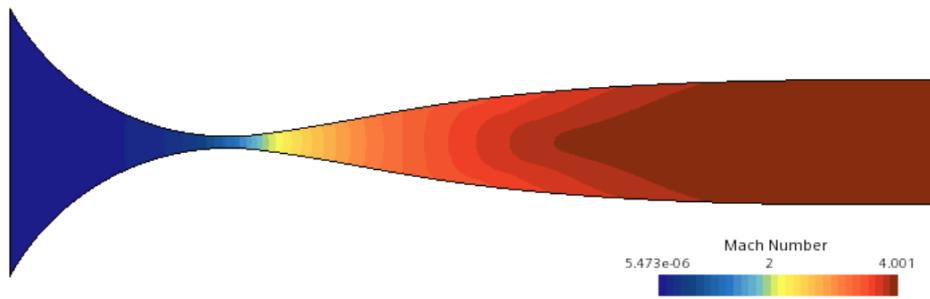
Figure 5.2: Inviscid contour for Mach 4.0 profile under inviscid simulation
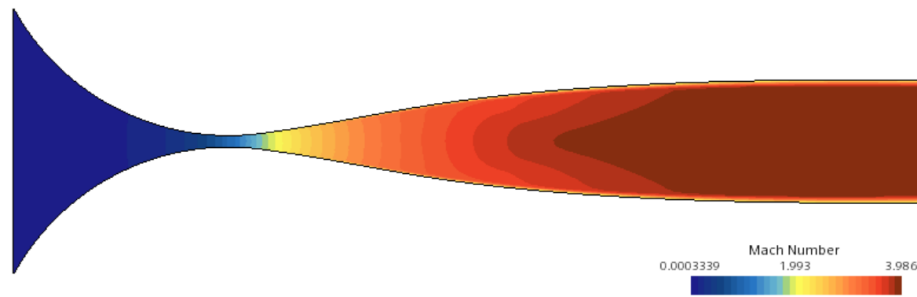
Figure 5.3: Inviscid contour for Mach 4.0 profile under viscous conditions

- Mach 5.0
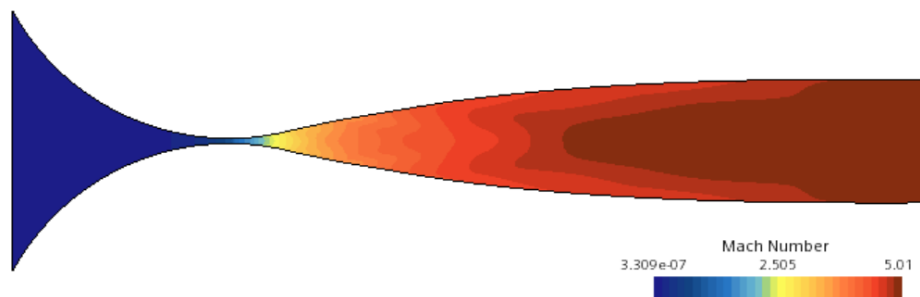
Figure 5.4: Inviscid contour for Mach 5.0 profile under inviscid simulation
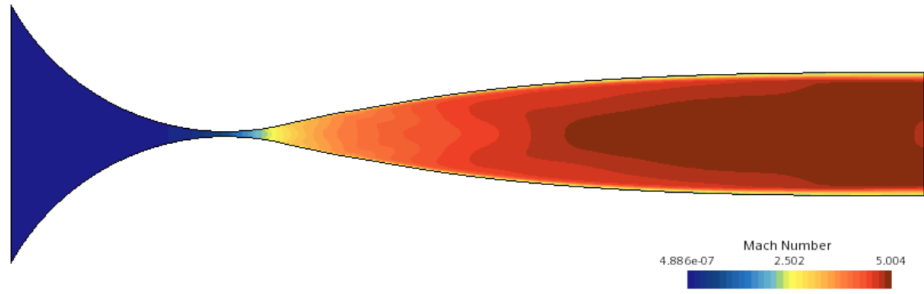
Figure 5.5: Inviscid contour for Mach 5.0 profile under viscous conditions

- Mach 6.0
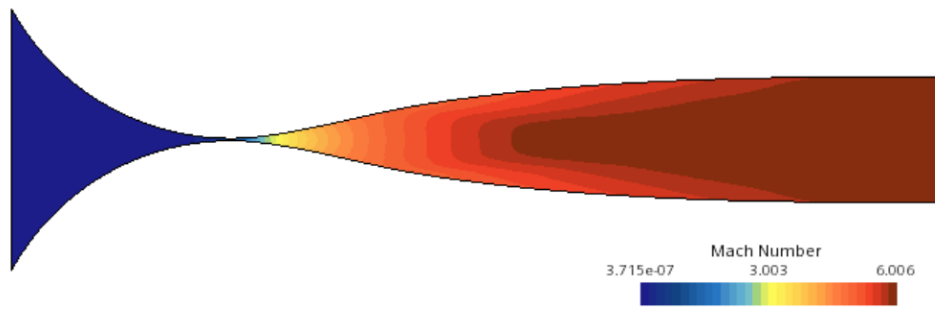
Figure 5.6: Inviscid contour for Mach 6.0 profile under inviscid simulation
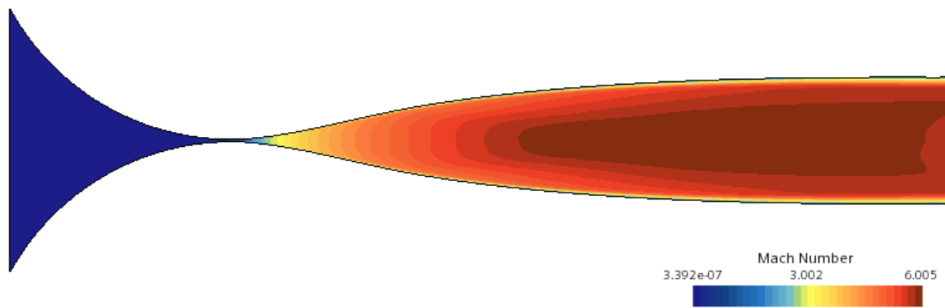
Figure 5.7: Inviscid contour for Mach 6.0 profile under viscous conditions

The inviscid simulation is observed to achieve the desired Mach numbers for all three contours, but once that same contour is simulated under viscous conditions, there are observable irregularities in the flow quality. There was a deficiency in achieving the designated Mach number which was expected. After analyzing each nozzle, a boundary layer thickness was calculated to apply the BLC to generate the optimized contour. See Table 5.1.

Table 5.1: Boundary layer thickness at outlet

Mach number	Boundary layer thickness at the outlet (in)
4.0	2.02
5.0	3.51
6.0	3.75

The values from table 5.1 were implemented to realize the BLC in each contour, generating a new one. These contours are depicted in Figures 5.8 – 5.10.
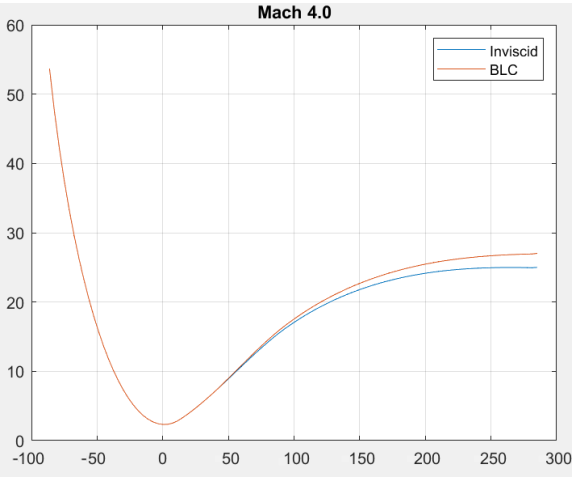
Figure 5.8: Boundary layer correction (BLC) applied to the Mach 4.0 nozzle
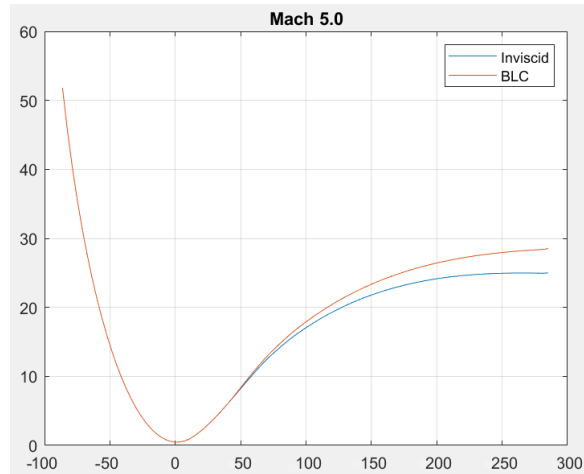
Figure 5.9: Boundary layer correction (BLC) applied to the Mach 5.0 nozzle
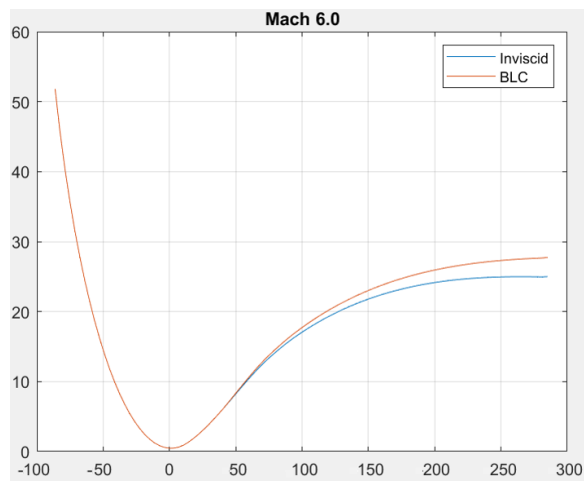
Figure 5.10: Boundary layer correction (BLC) applied to the Mach 6.0 nozzle

5.2. Steady-State Viscous Contour

After applying the BLC to the nozzle contours a new simulation was created for each one producing the following results:

- Mach 4.0
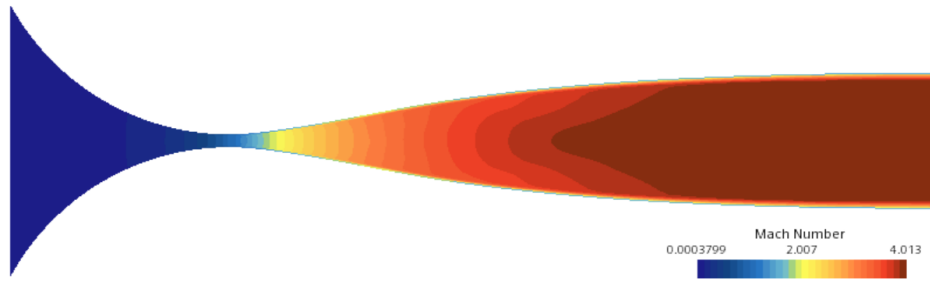
Figure 5.11: Optimized nozzle contour for Mach 4.0

- Mach 5.0
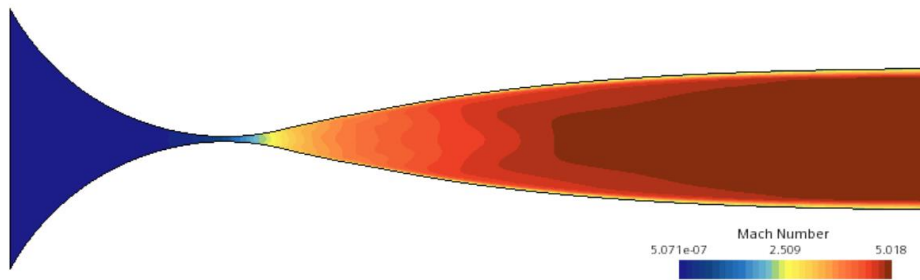
Figure 5.12: Optimized nozzle contour for Mach 5.0 profile

- Mach 6.0
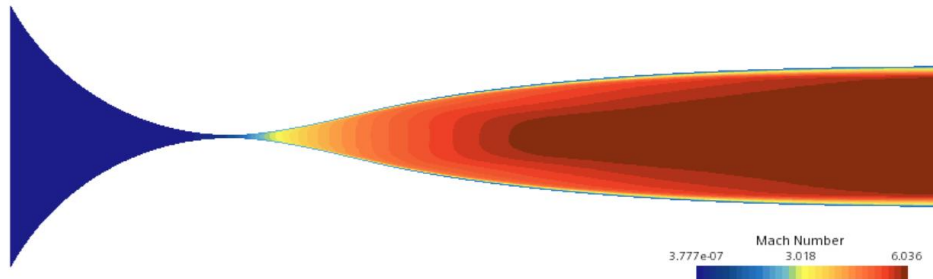
Figure 5.13: Optimized nozzle contour for Mach 6.0 profile

5.3. Transient Analysis

The transient analysis was implemented to observe the transient effects that might be presented in real life conditions. Once expansion starts the flow begins to develop and oblique shocks are generated due to the high-speed conditions. The boundary layer starts generating and ultimately the flow begins to straighten creating uniform flow at the most downstream section of the nozzle.

- Mach 4.0
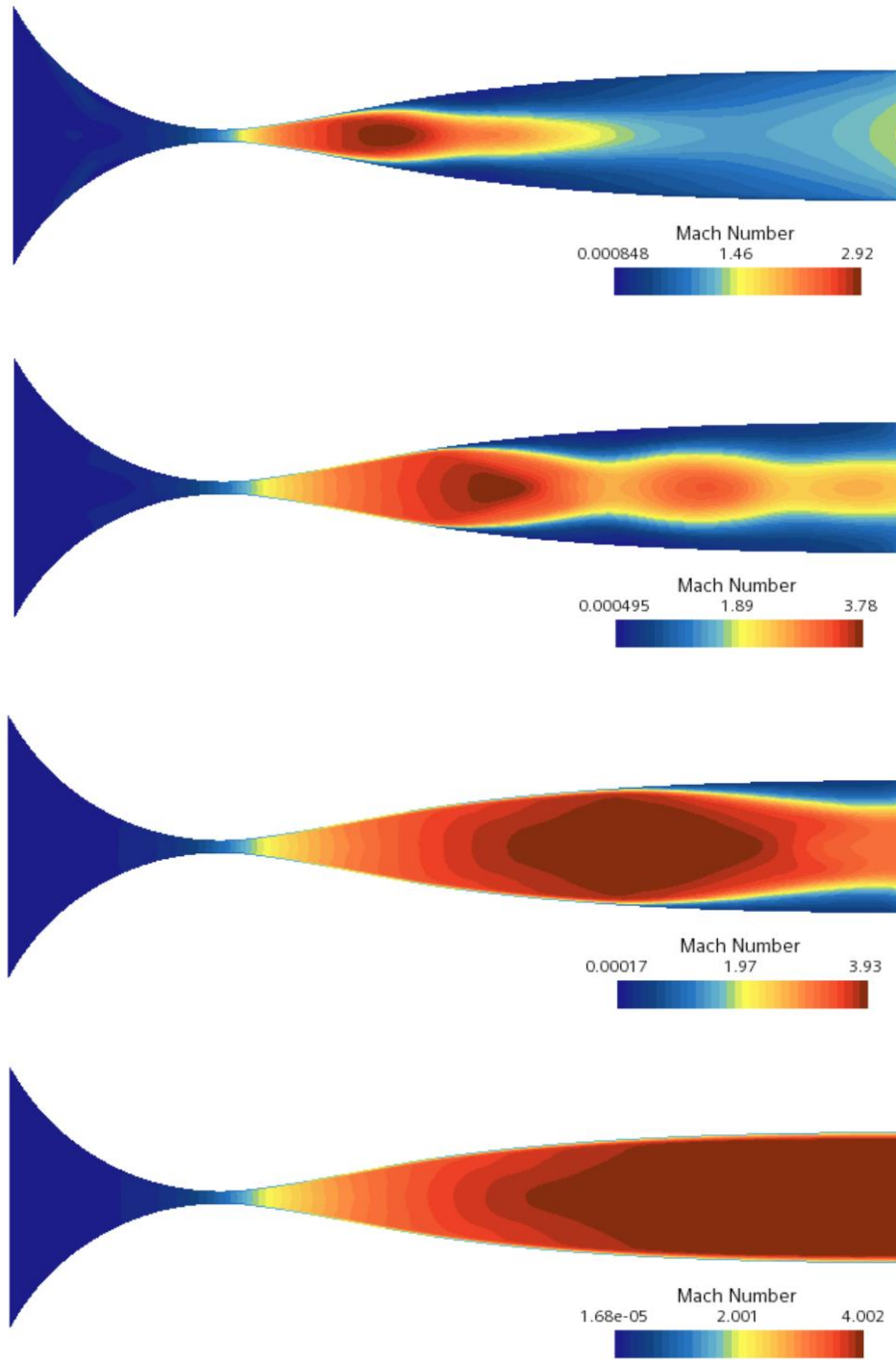
Figure 5.14: Mach 4.0 transient profile

- Mach 5.0
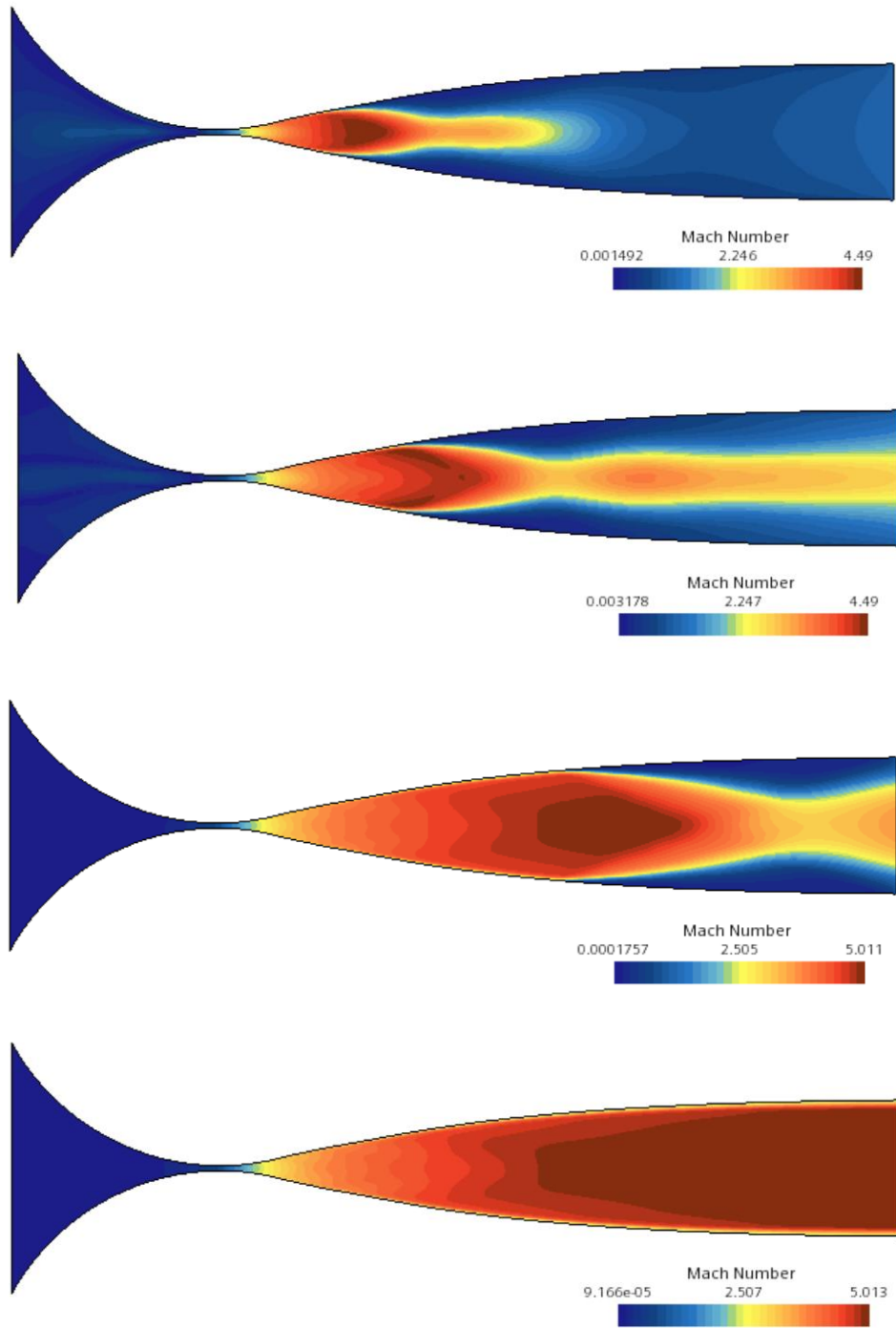
Figure 5.15: Mach 5.0 transient profile

- Mach 6.0
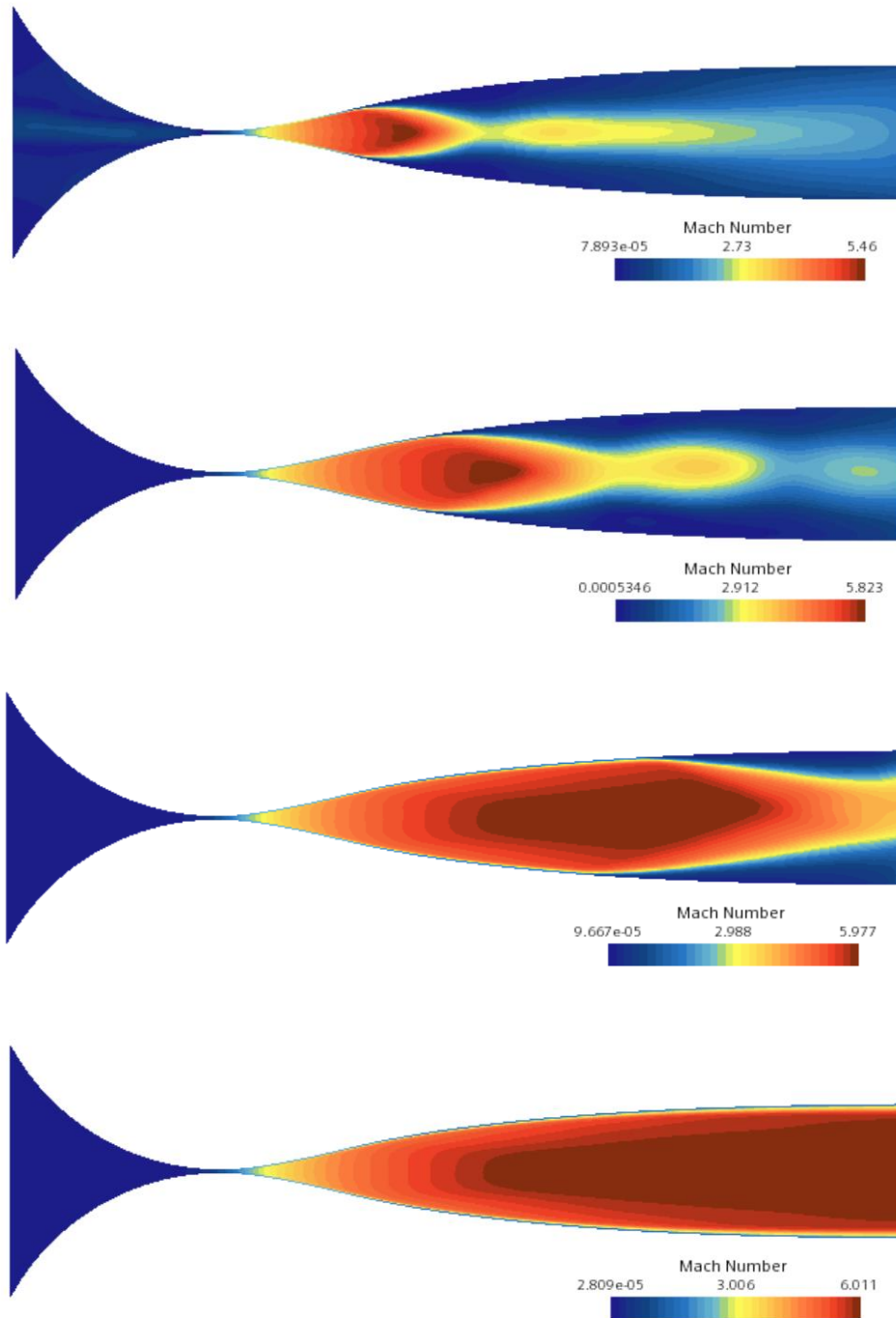
Figure 5.16: Mach 6.0 transient profile

Each nozzle exhibits similar behavior, showcasing the flow separation from the walls and causing these oblique shapes. The expansion can be observed in the expansion section and it is gradually straightened once it moves further downstream and achieves a uniform flow achieving the desired Mach number for each respective contour.

6. Conclusion

Supersonic processes become challenging due to various phenomena that develop at these speeds. Convergent-divergent nozzles are designed to reproduce such velocities and serve as an enclosed domain for aerodynamic testing. The challenges of this type of nozzle begin in its design and what appropriate measures should be considered to satisfy supersonic or hypersonic conditions. The method of characteristics proves to be a robust methodology for the generation of supersonic nozzle geometries. The complexities encountered in crafting such geometries inquire the necessity of implementing isentropic relations within the realm of compressible flows. By characterizing the principal conditions of the nozzle using the obtained isentropic parameters this can easily facilitate the design process.

Two fundamental factors are essential to design a supersonic nozzle using the MoC: maximum expansion angle, and isentropic equations. These are practically required to achieve the desired Mach number and must be satisfied. This study implemented a maximum expansion angle lower than that of equation 2.19 by a substantial amount, due to the gradual expansion requirement, the values assigned were found to be useful to design the nozzles. The isentropic parameters were respected by assigning a fixed dimension at the outlet and considering the aspect ratio between parameters to find the required inputs.

The corresponding parameters for each Mach number design aided in the formulation of appropriate solver, mesh, and boundary conditions for the simulations to perform as efficiently. The manipulation of the inviscid contours to adapt the boundary layer correction (BLC) and optimizing the contour by calculating the boundary layer thickness was effectively applied, culminating in the total convergence of all three nozzles.

It is noteworthy that this analysis extends to the hypersonic regime, where the control of airflow becomes notably more challenging. The variations in the flow behavior, as evidenced in Figures 5.7 – 5.9 reveal the performance at Mach 5.0 and 6.0 is comparatively less favorable than Mach 4.0. But the designed Mach numbers were achieved thanks to the BLC applied to the inviscid

contour. The difficulty in flow development at higher Mach numbers is due to the minimizing in the cross-sectional at the throat region. The higher the Mach number the smaller the throat, hence the flow struggles to pass through due to that minuscule space.

Separately, the transient process for each nozzle presented a characteristic visualization of what occurs inside a supersonic nozzle. This introduces an integral aspect of how a nozzle operates under these conditions and aids in the development of future applications by understanding and determining the main aerodynamic behaviors that need to be considered in high-speed regimes.

7. Recommendations for Future Applications

7.1. Sivells' Method

Sivells' nozzle design is perhaps the most recent direct design MoC-based method. Figure 7.1 demonstrates the integrity of Sivells code, showing the requirements to obtain a uniform flow nozzle contour aided by having a radial flow region with two different centerline Mach number distributions accompanied by the MoC.
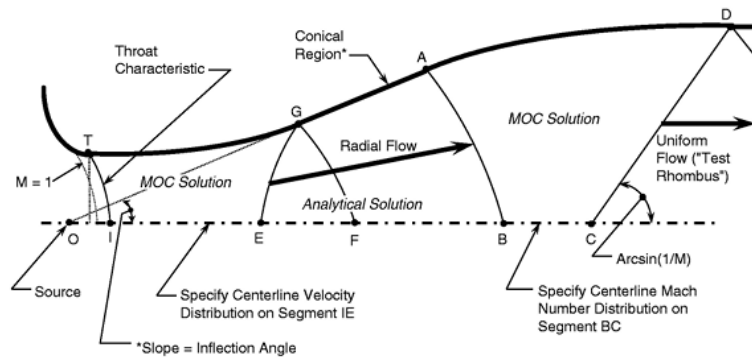
Figure 7.1: Notation and design procedure used by Sivells (Shope, 2005)

On the other hand, as an option, a single centerline Mach number distribution can be used as seen in Figure 7.2, ignoring the radial source flow involvement.
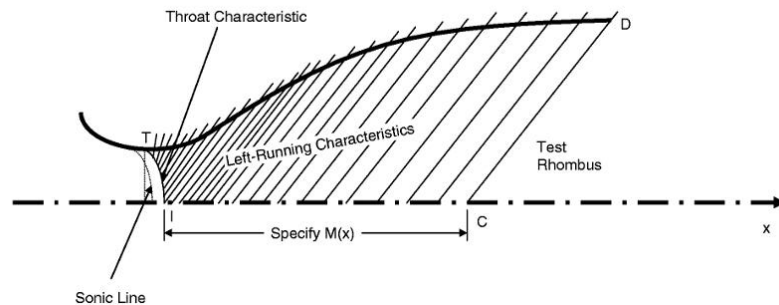
Figure 7.2: Sivells' second option for nozzle design (Shope, 2005)

The highest flow quality is obtained with a radial flow region, but the result of using this method lies in the consequence that the nozzle must constitute a substantial longitude to satisfy the uniform flow at the exit. Both options require a circular throat that is mathematically calculated to perfectly align with the expanding curvature and obtain a gradual transition between the throat, radial source, and nozzle exit flow. Sivells aimed to produce an accurate nozzle design by setting distinct parameters to determine the contour of the nozzle with a respective cubic spline polynomial by initially interpreting inviscid conditions and computationally interfacing the continuum into a viscous regime that will incorporate a boundary layer with the purpose of optimizing the nozzle's contour to generate the most efficient design and capture the desired Mach number (Shope, 2005).

References

[Anderson, J. D., Cadou, C. P. 2023. Fundamental of Aerodynamics, Seventh Edition, McGraw Hill LLC]

[Anderson, J. D. 2020. Modern Compressible Flow: With Historical Perspective, Fourth Edition, McGraw-Hill Education]

[Ansys Innovation Courses. 2020. Method of Characteristics – Lesson 6 https://courses.ansys.com/index.php/courses/internal-compressible-flows/lessons/method-of-characteristics-lesson-6/]

[Cengel, Y. A., Cimbala, J. M. 2017. Fluid Mechanics Fundamentals and Applications]

[Deng, Y. 2018. Design of a Two-Dimensional Supersonic Nozzle for use in Wind Tunnels]

[John, J., Keith, T. 2006. Gas Dynamics. Pearson Prentice Hall]

[Khan, M. A., Sardiwal, S. K., Sharath, M. V. S., Chowdary, D. H. 2013. Design of a Supersonic Nozzle using Method of Characteristics]

[Kim, S., Kim, S. D., Jeung, I., Lee, J., Choi, J. 2014. Boundary Layer Correction of Hypersonic Wind-Tunnel Nozzle Designed by the Method of Characteristics]

[NASA Glenn Research Center. n.d. Isentropic Flow https://www.grc.nasa.gov/www/BGH/isentrop.html]

[Ogawa, H., Matsunaga, M., Fujio, C., Higa, Y., Handa, T. 2022. Nozzle design optimization for supersonic wind tunnel by using surrogate-assisted evolutionary algorithms]

[Pope, A, Goin, K. L. 1965. High-Speed Wind Tunnel Testing, Wiley]

[Princeton University, n.d. Definition of Viscosity https://www.princeton.edu/~gasdyn/Research/T-C_Research_Folder/Viscosity_def.html

[Shapiro, A.H. 1953. The Dynamics and Thermodynamics of Compressible Fluid Flow, Vol. 2, Ronald Press Company]

[Shope, F. L. 2005. Design Optimization of Hypersonic Test Facility Nozzle Contours Using Splined Corrections]

[Siemens Digital Industries Software. 2021 Simcenter STAR-CCM+ User Guide https://docs.sw.siemens.com/documentation/external/PL20200227072959152/en-US/userManual/userGuide/html/index.html]

[Sivells, J. C. 1978. A Computer Program for the Aerodynamics Design of Axisymmetric and Planar Nozzles for Supersonic and Hypersonic Wind Tunnels]

[Vallabh, B. 2016. Investigation of Nozzle Contours in the CSIR Supersonic Wind Tunnel]

[Zucrow, M. J., Hoffman, J. D. 1977. Gas Dynamics: Multidimensional Flow, Vol. 2, Wiley]
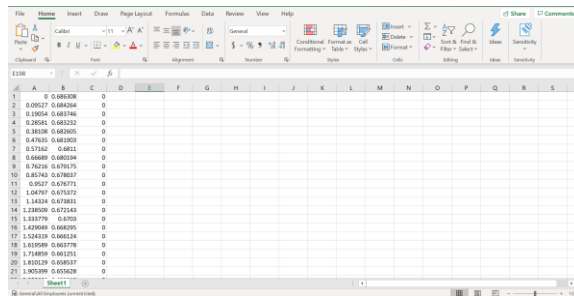
Appendix

STEADY STATE COMPREHENSIVE SIMULATION SETUP

This setup will describe how to configure STAR-CCM+'s environment to create the simulation for this project in a step-by-step process.

a. Coordinates

1. Open an Excel file and input the coordinates for the nozzle in xyz format. (A=x, B=y, and C=z)

2. Since this is a 2D simulation, the column for z is 0

3. Make sure to use the same units throughout the entire process to minimize mistakes. Here the coordinates are in meters

4. Save the file as a Comma Separated Values file (.csv) (use meters)

b. Create a New STAR-CCM+ File

5. Open Star-CCM+

6. At the left top corner click on the paper-with-a-plus-sign icon
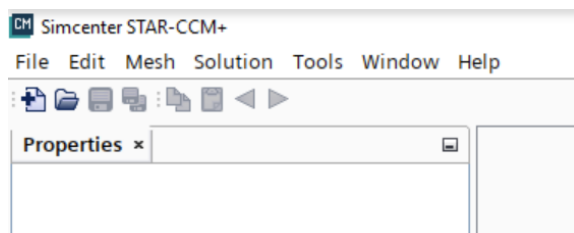
7. On the new tab, select "Parallel on Local Host" and enter 4 in "Compute Processes". This value is dependent on your computational equipment.

8. Click "OK"
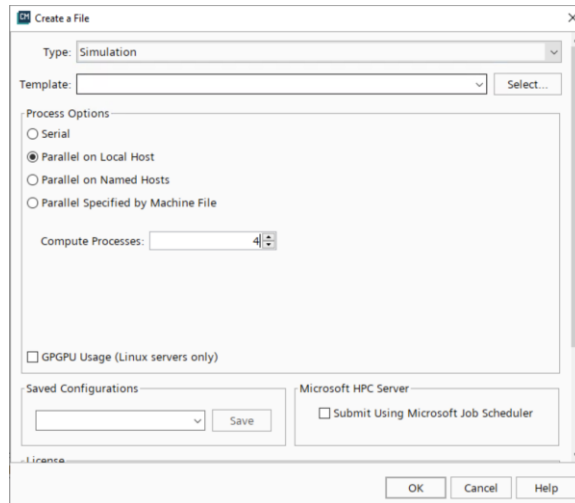
c. **3D-CAD Workspace**

9. Expand "Geometry" section

10. Right click "3D-CAD Models"

11. Select "New" (this will open your workspace to create your model)
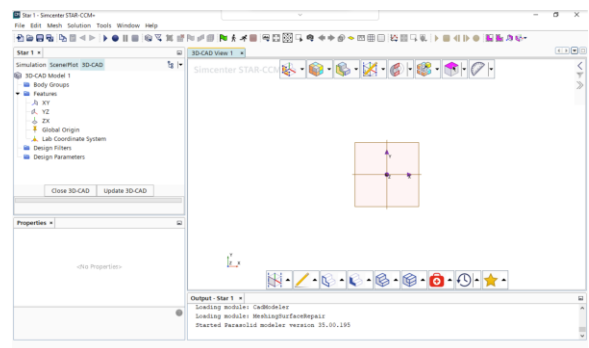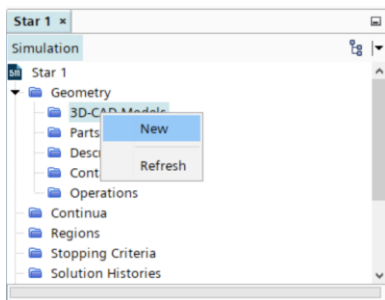
d. **Import Coordinates**

12. Right Click on "3D-CAD Model 1"

13. Select "Import"

14. Select "3D Curves"
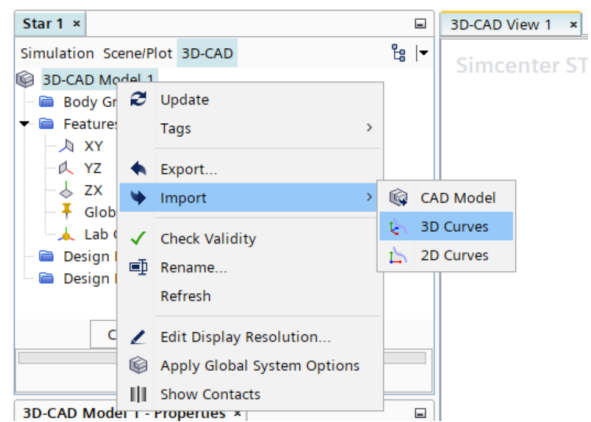
15. Select the csv file created

16. Click on "Open"

17. Select "Import as polyline" (this connects each coordinate point together with a straight line between each point

18. Checkmark on "Close the curve" to close the generated polyline

19. Click "OK"
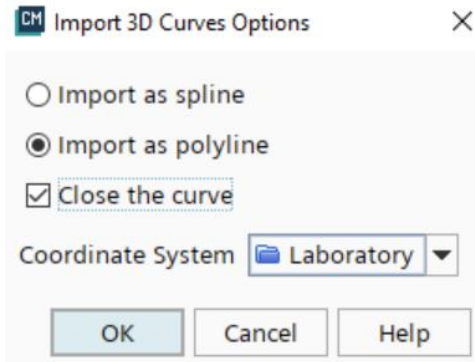
e. Create CAD

20. Right click on "Sketch3D 1"

21. Select "Extrude"
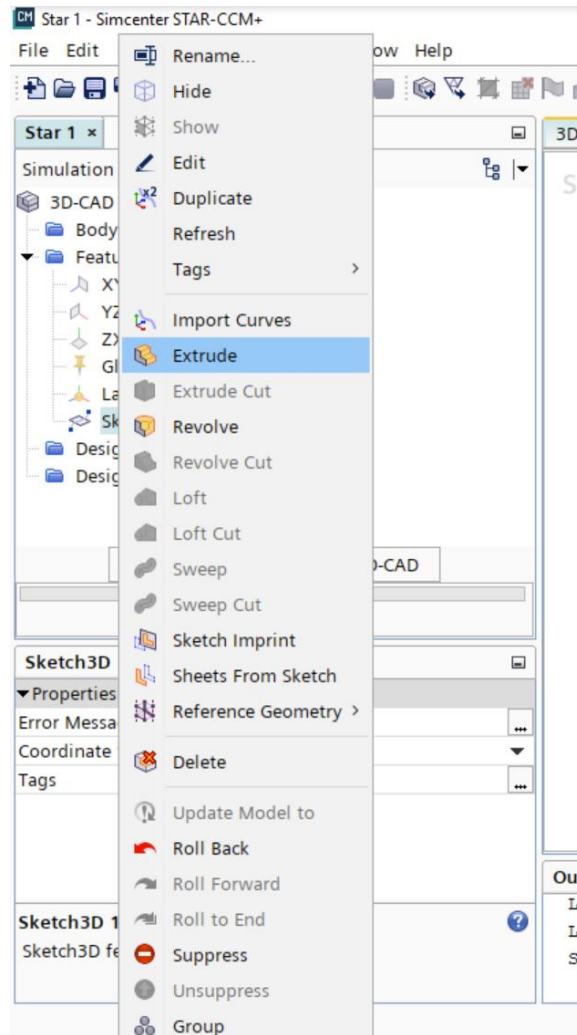
22. Since this process creates a 2D simulation there is no need to specify the extrusion distance but to ease the next step when selecting the different boundaries this value can increased in "Distance"

23. Click "OK"
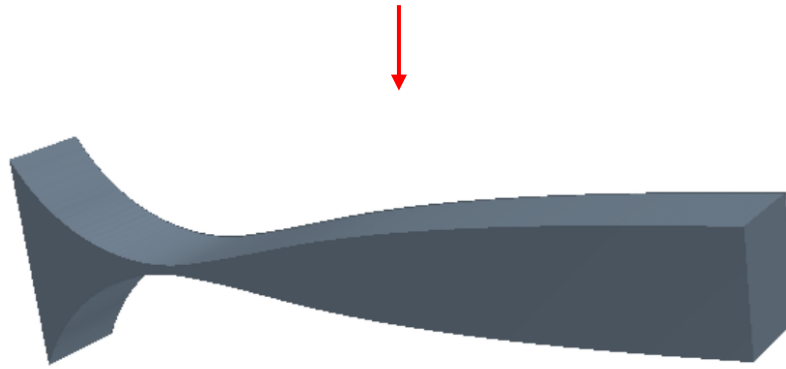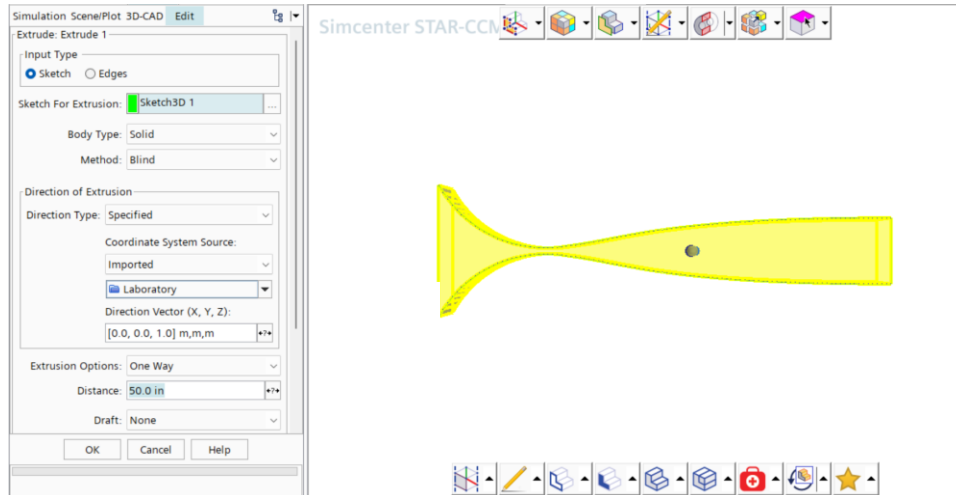
f. Assign Name to Regions/Faces

24. First name the component by right clicking on "Body 1" or the desired part

25. Select "Rename"

26. Type "Nozzle" or desired name
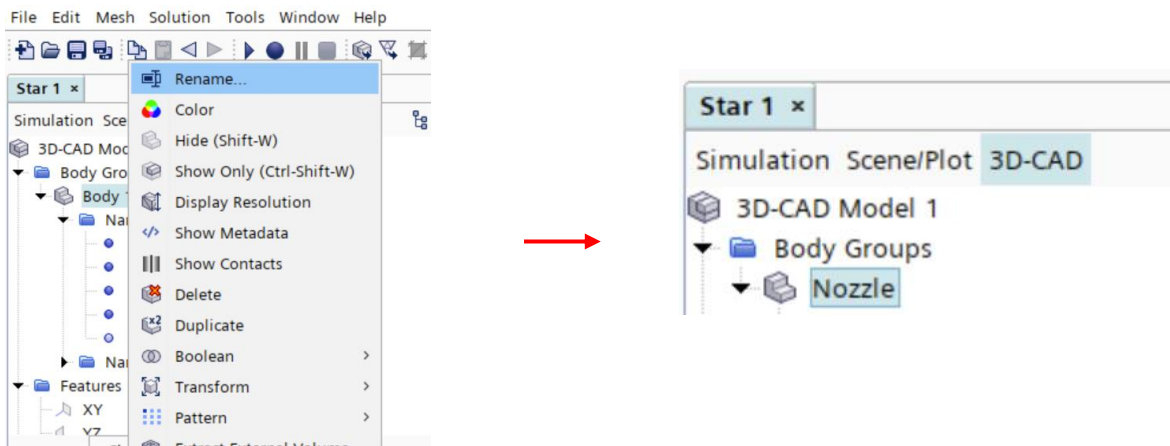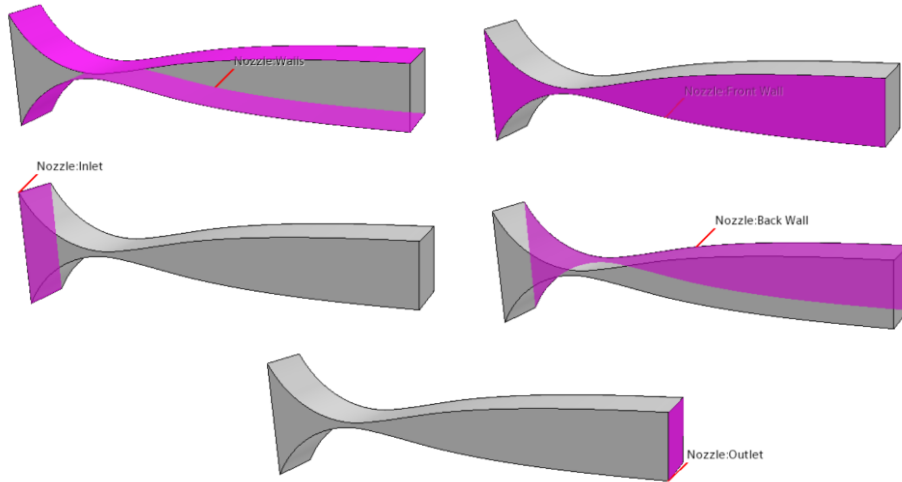
27. Right click on each of the faces

28. Select "Rename"

29. Name the face and click "OK"
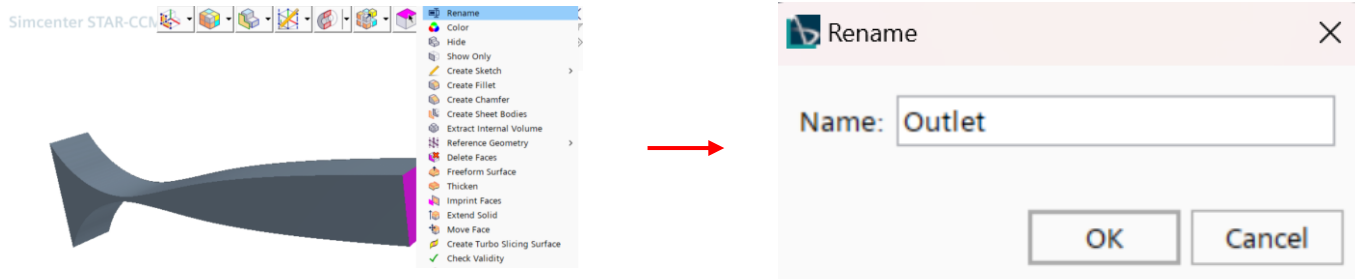
30. Repeat previous step for Inlet and Walls

Note 1: Front Wall and Back Wall are named separately due to the 2-dimensional requirement of the simulation. This will allow the continuum to select one of these faces to act as the 2D geometry field when running the solution.

g. **Exit 3D-CAD Workspace**

31. Click "Close 3D-CAD"
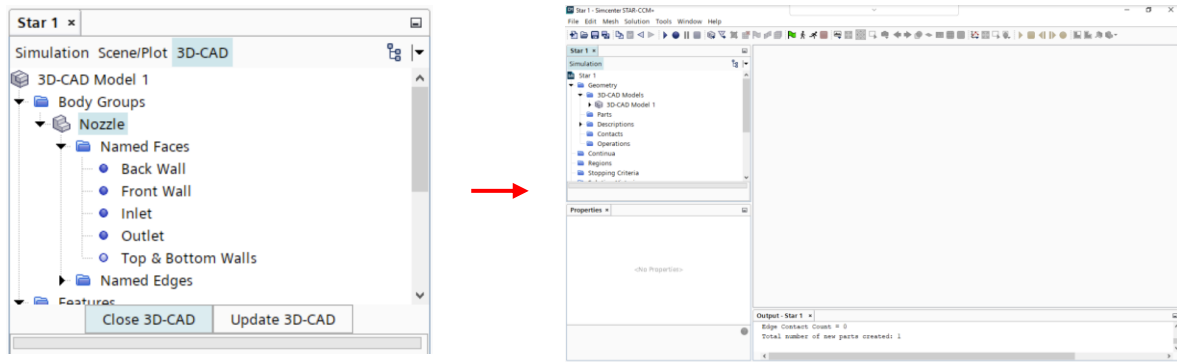
h. **Generate Geometry for Simulation**

32. Expand "3D-CAD Model 1" section

33. Expand "Body Groups" section

34. Right click on "Nozzle"

35. Select "New Geometry Part"
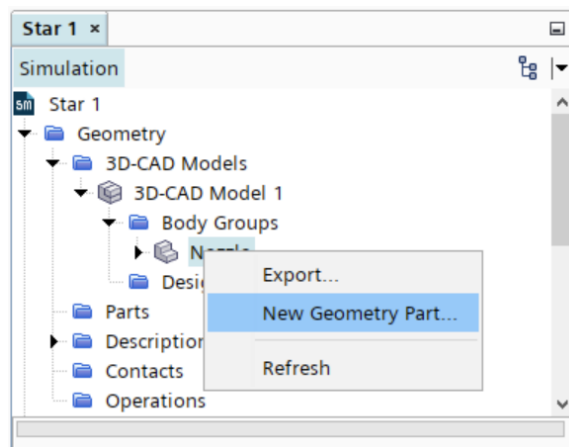
36. Select "OK"
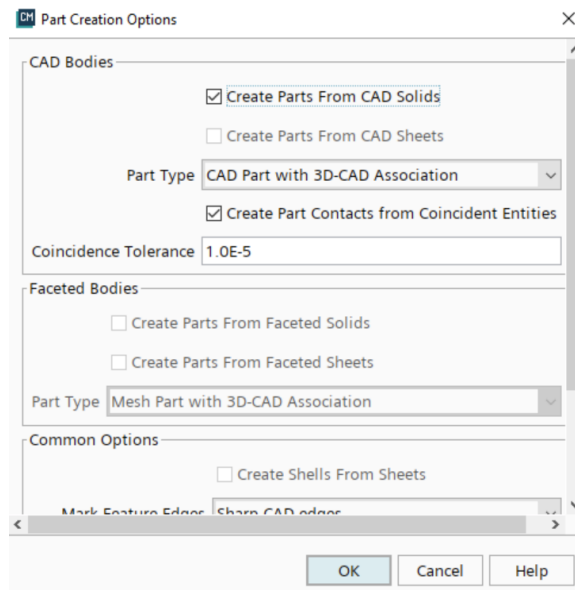
i. **Assign 2D Mesh Configurations**

37. Right click on "Operations"

38. Select "New"

39. Select "Mesh"

40. Select "Badge for 2D Meshing"
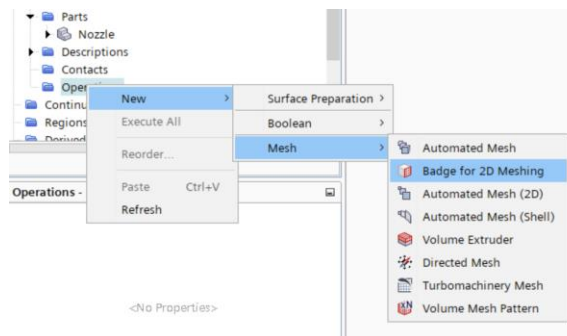
41. Select part ("Nozzle")

42. Checkmark "Execute Operation Upon Creation"

43. Click "OK"
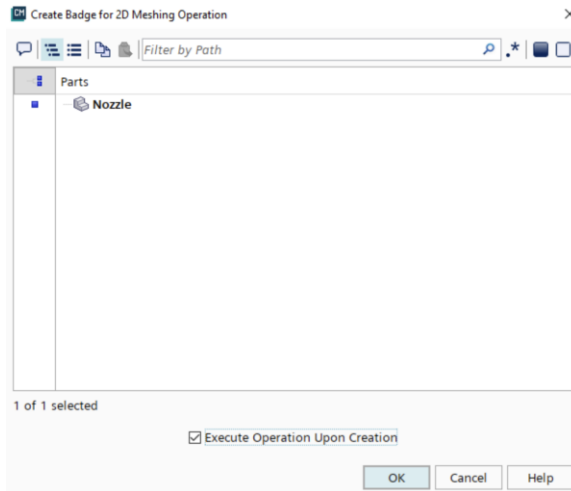
Note 2: *for 2D models the "Badge for 2D Mesh" feature is required to generate the needed boundaries for the continuum in 2D. As specified in Note 1, the lateral walls of the nozzle must be identified separately for this to work and generate the 2D geometry. Once the feature is executed the Nozzle "Surfaces" section must appear as follows":*
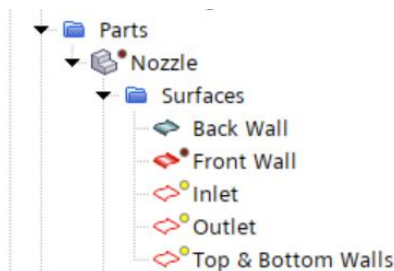
j. Assign Parts to Regions

44. Expand "Parts" section

45. Right click on "Nozzle"

46. Select "Assign Parts to Regions"
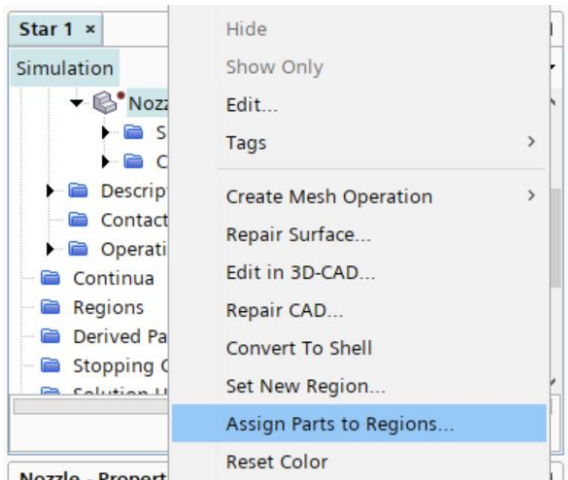
47. Select "Create a Region for Each Part"

48. Select "Create a Boundary for Each Part Surface"

49. Click "Apply"

50. Click "Close"
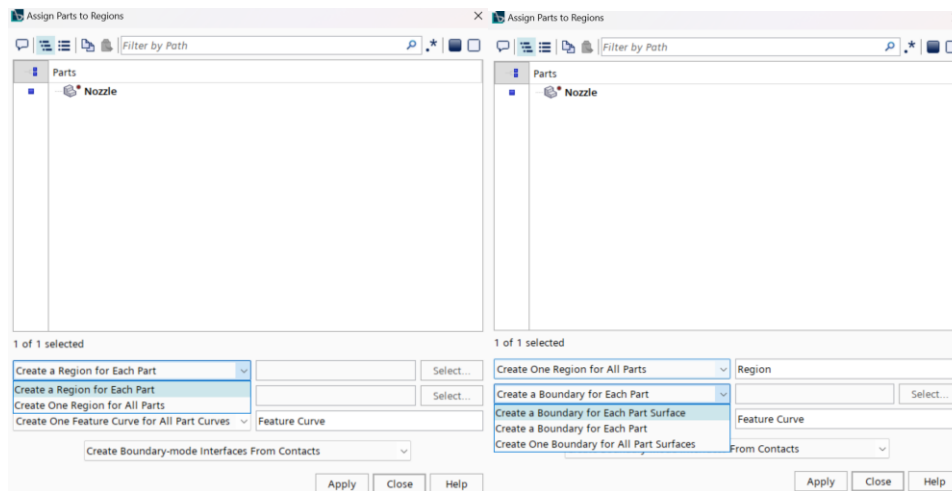
k. Assign Boundary Conditions

51. Expand "Regions" section

52. Expand "Nozzle" section

53. Expand "Boundaries" section

54. Assign boundary type to each boundary:

- Inlet: Stagnation Inlet

- Outlet: Pressure Outlet

- Walls: Wall
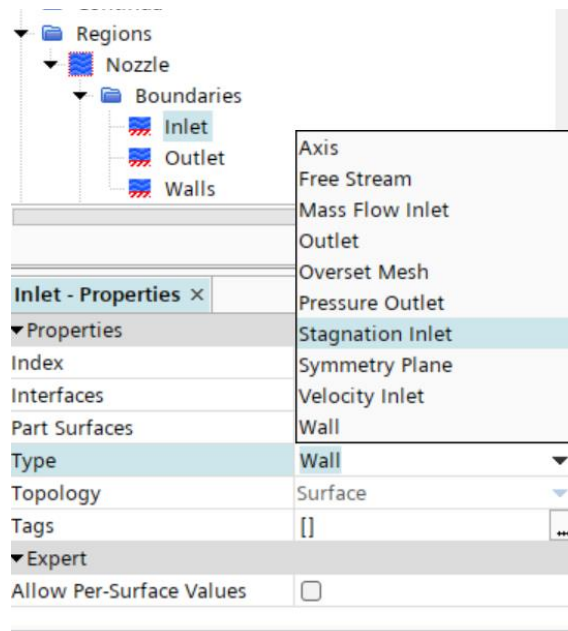
l. Generate Mesh

55. Right click on "Operations"

56. Select "New"

57. Select "Mesh"

58. Select "Automated Mesh (2D)"
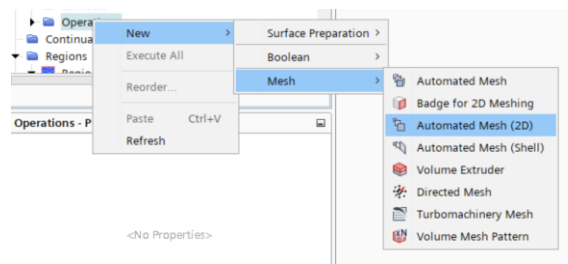
59. Select part ("Nozzle")

60. Select Meshers

- Polygonal Mesher

- Prism Layer Mesher

61. Click "OK"
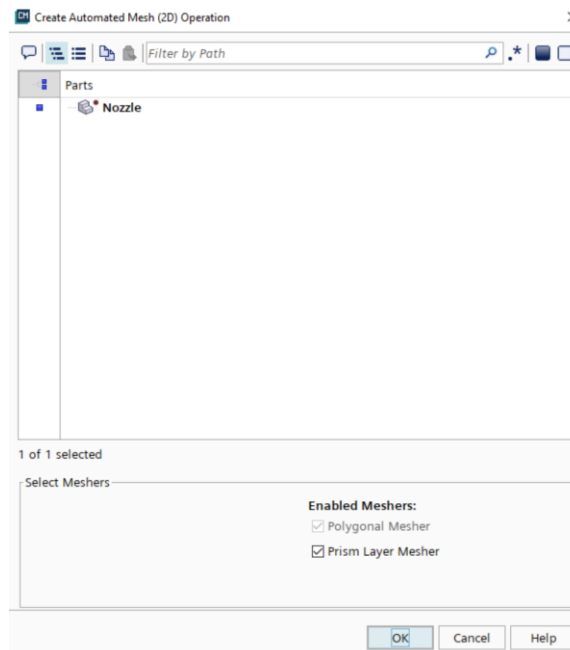
Base Size

62. Expand "Automated Mesh (2D)" section

63. Expand "Default Controls"

64. Select Base Size

65. Set base size to 1.0 in
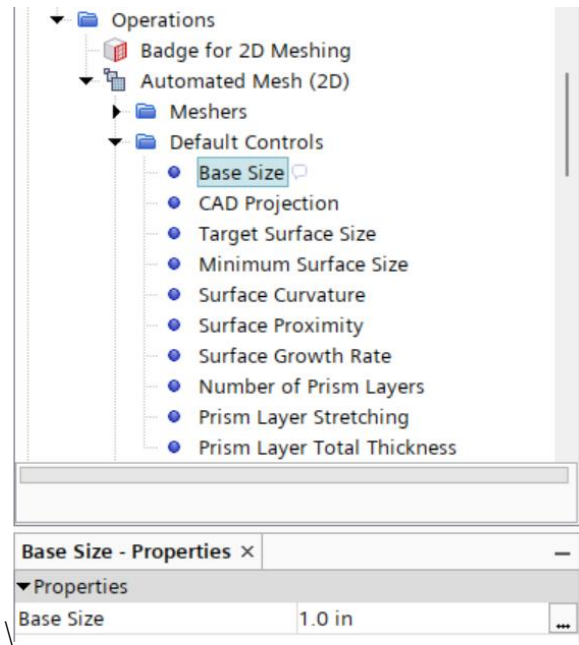
Surface Growth Rate

66. Select "Surface Proximity"

67. Set "# Points in gap" to 5.0. This will apply more cells throughout the throat area.
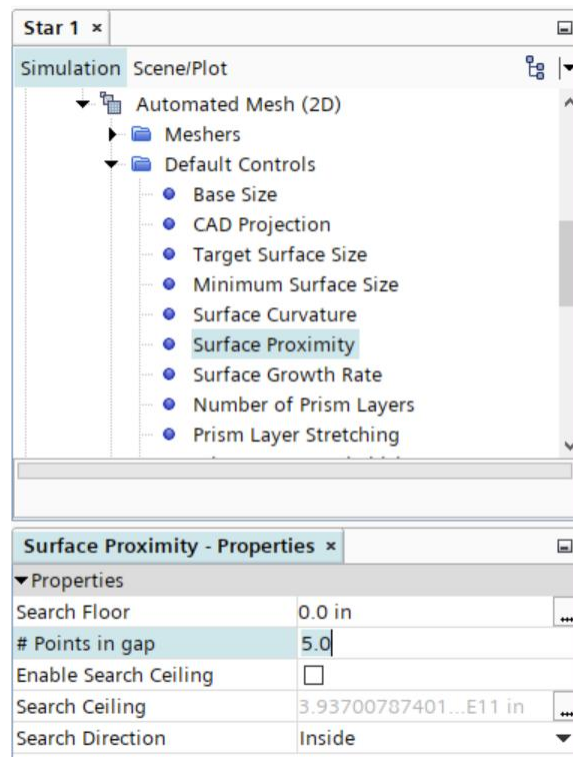
68. Select "Surface Growth Rate"

69. Set "Surface Growth Rate" to Slow
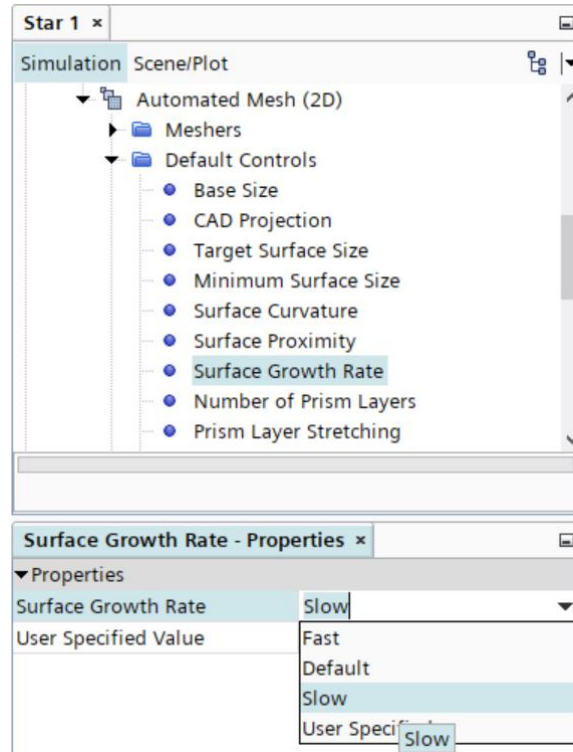
Prism Layer Stretching

70. Select "Number of Prism Layers"

71. Set "Number of Prism Layers" to 10
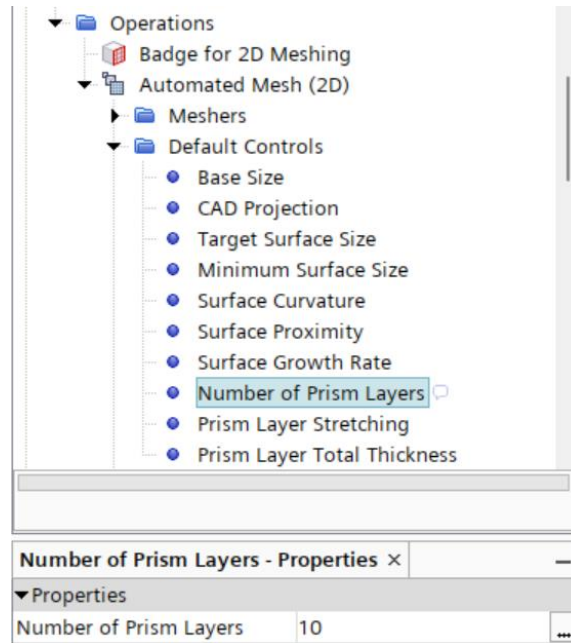
72. Select "Prism Layer Stretching"

73. Set "Prism Layer Stretching" to 1.3
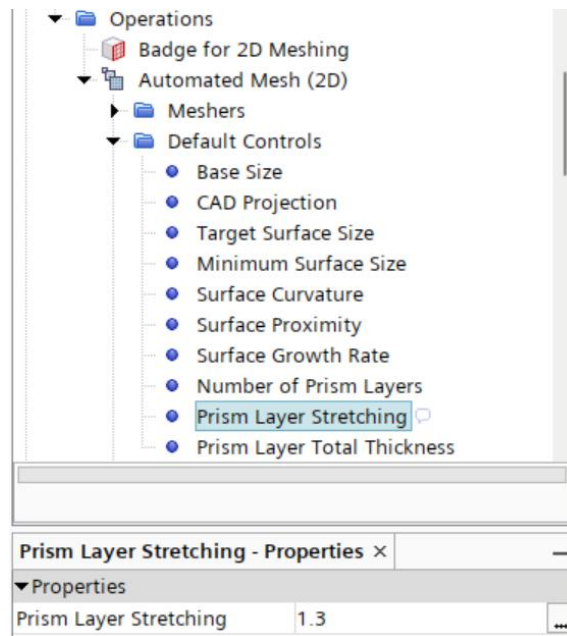
Prism Layer Total Thickness

74. Select "Prism Layer Total Thickness"

75. Set Size Type to "Absolute"

76. Set "Absolute Size" to 4.0 in
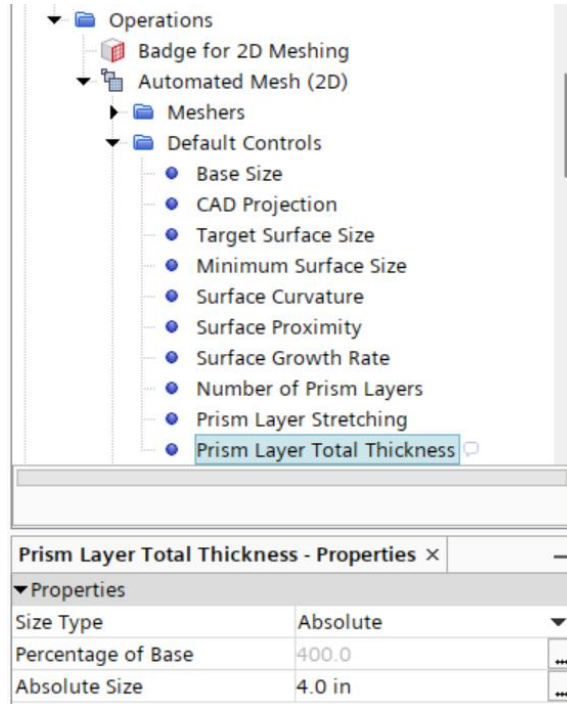
Note 3: the Absolute Size of the prism layer is initially set to 4.0 in for the inviscid solution as described in section 4.2. This value must be changed respectively for Mach 4.0, 5.0, and 6.0.

Execute Mesh

77. Right click on "Automated Mesh (2D)

78. Select "Execute"
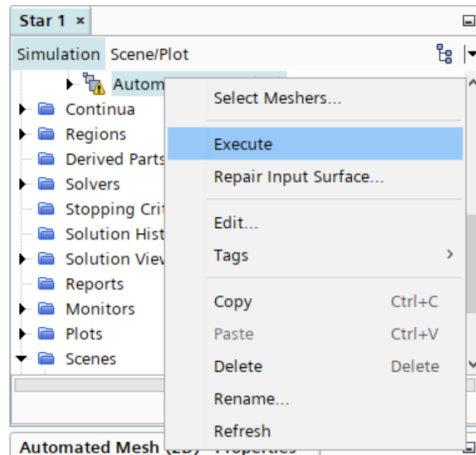
m. Physics Continua

79. Expand "Continua" Section

80. Select "Select Models"
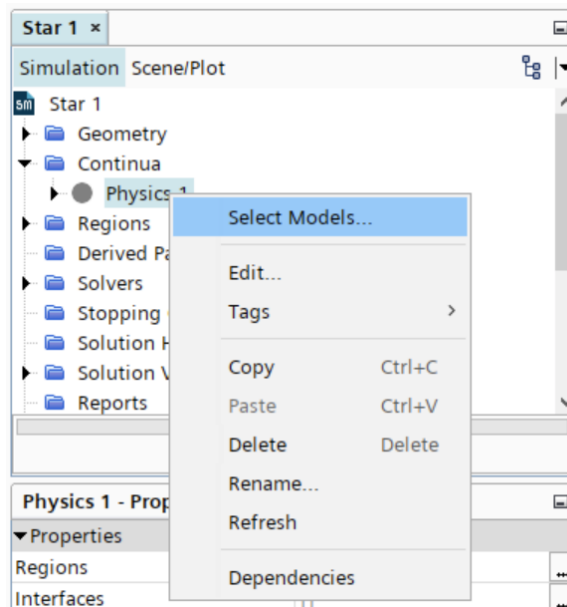
81. Select the following:

- Time: Steady

- Material: Gas

- Flow: Coupled Flow

- Equation of State: Ideal Gas

- Viscous Regime: Turbulent

- Reynold-Averaged Turbulence: K-Epsilon Turbulence

- Click on "Close"
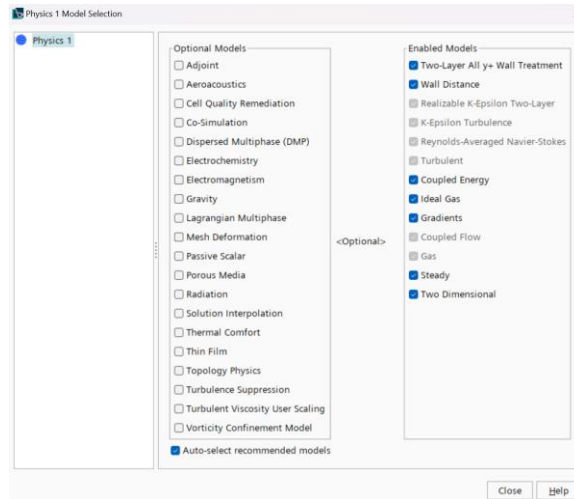
Inviscid Flux

82. Expand "Physics 1" Section

83. Expand "Models" section

84. Select "Coupled Flow"

85. Change "Coupled Inviscid Flux" to AUSM+ FVS
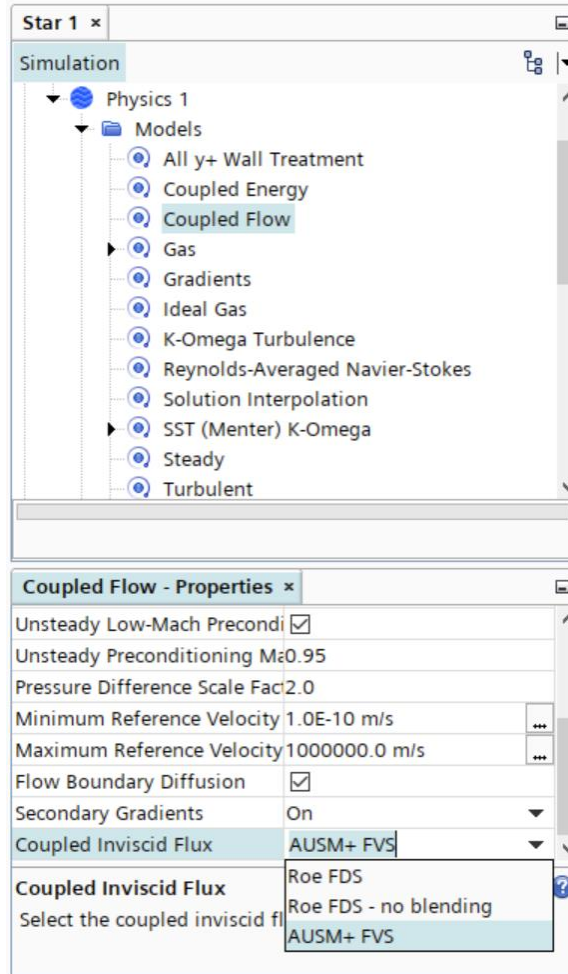
Material Properties

86. Expand "Gas" section

87. Expand "Air" section

88. Expand "Material Properties" section

89. Select "Dynamic Viscosity"

90. Set method to "Sutherlands Law"
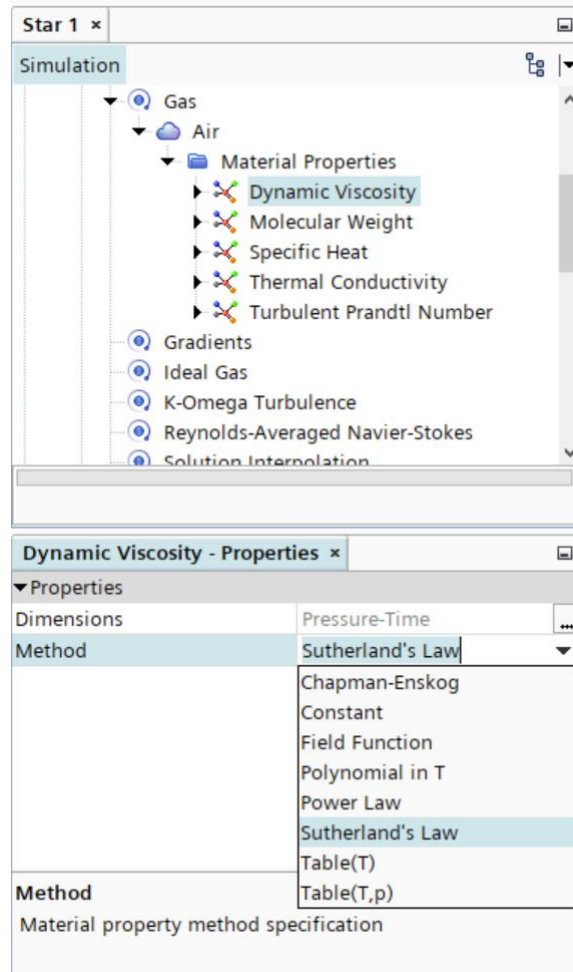
Reference Values

91. Expand "Reference Values" section

92. Set the following (Mach 4.0):

- Reference Pressure: 0 psi

- Minimum Allowable Absolute Pressure: 1.91 psi

- Minimum Allowable Temperature: 129.76 R

- Maximum Allowable Absolute Pressure: 290 psi

- Maximum Allowable Temperature: 545 R
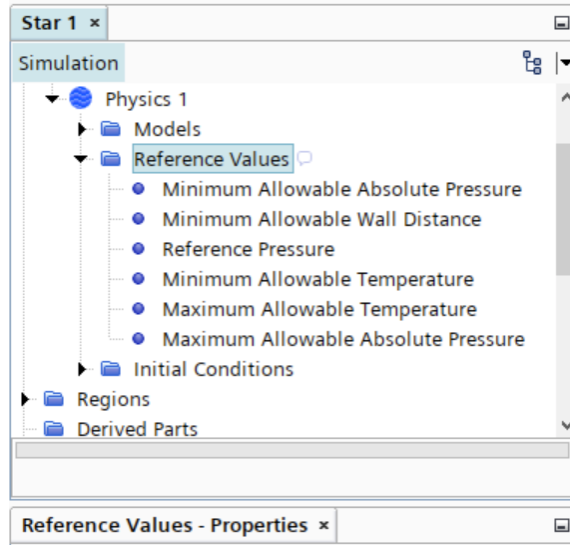
Note 4: *section 4.3.3 specifically defines the reference values for each Mach number. Change accordingly.*

Initial Conditions

93. Expand "Initial Conditions" section

94. Set the following (Mach 4.0):

- Pressure: 12.97 psi

- Static Temperature: 483.14 R

- Velocity: [274.4,0] m/s
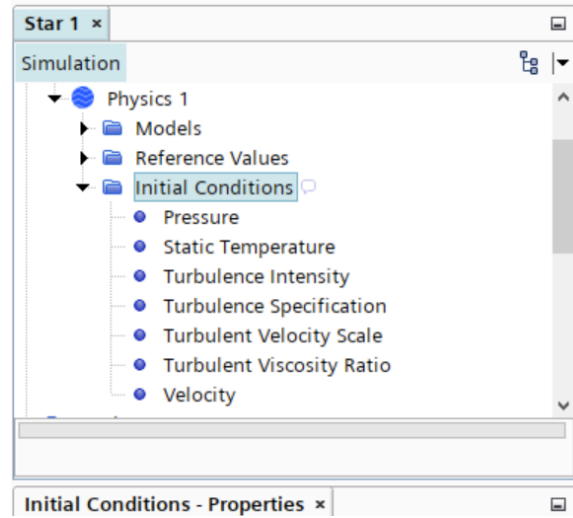
Note 5: these values are set to achieve an appropriate convergence. See section 4.3.2.

n. **Solvers**

95. Expand "Solver" section

96. Expand "Coupled Implicit"

97. Select "Automatic CFL"

98. Set "Initial CFL" to 1.0

99. Set "Maximum CFL" to 10
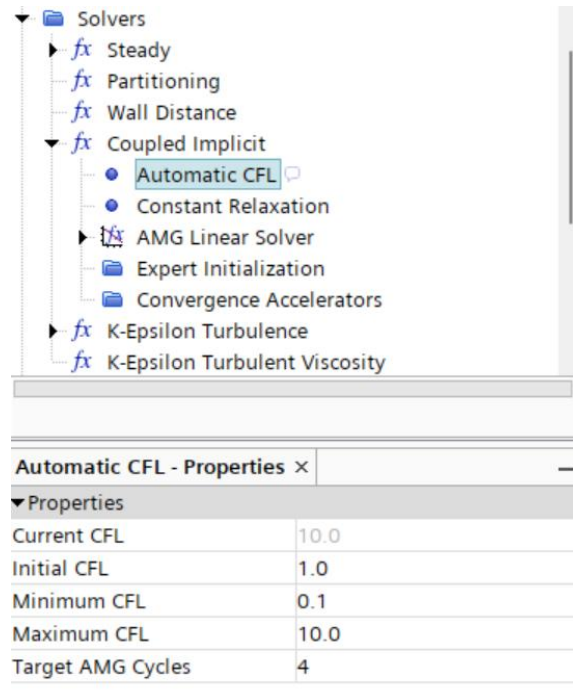
o. Boundary Inputs

100. Expand "Regions" section

101. Expand "Nozzle" section

102. Expand "Boundaries" section

Inlet

103. Expand "Inlet" section

104. Expand "Physics Values" section

105. Set the following:

- Supersonic Static Pressure: 1.91 psi

- Total Pressure: 290 psi

- Total Temperature: 545 R
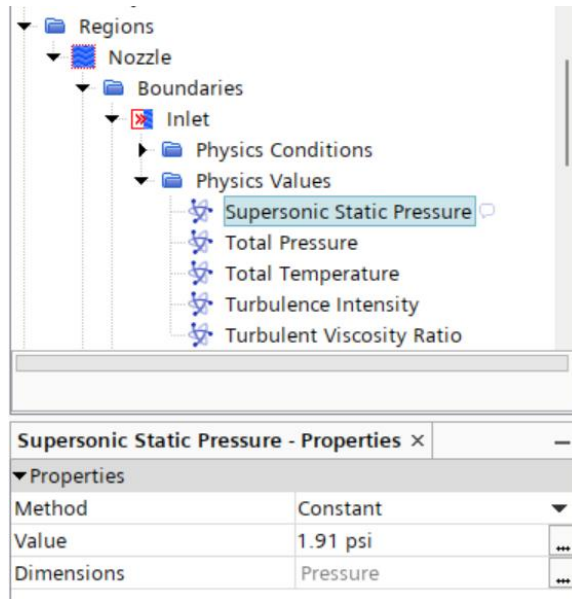
Outlet

106.   Expand "Outlet" section

107.   Expand "Physics Values"

108.   Set the following:

- Pressure: 1.91 psi

- Static Temperature: 129.76 R
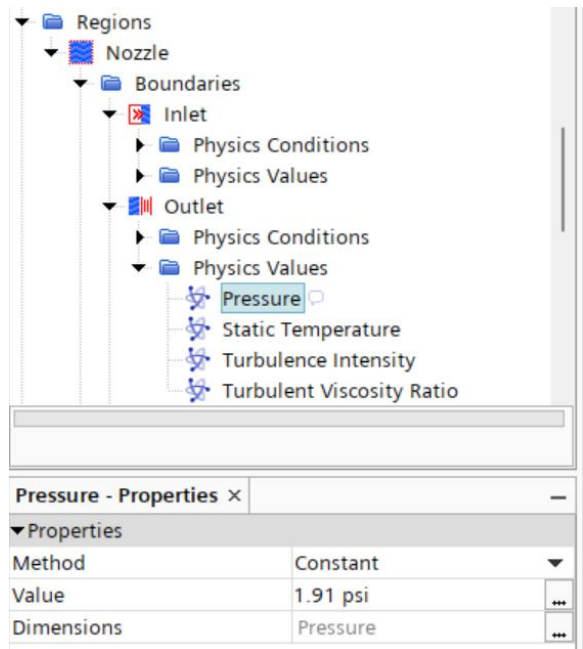
109. Expand "Physics Conditions"

110. Select "Backflow Specification"

111. For Pressure select "Static"
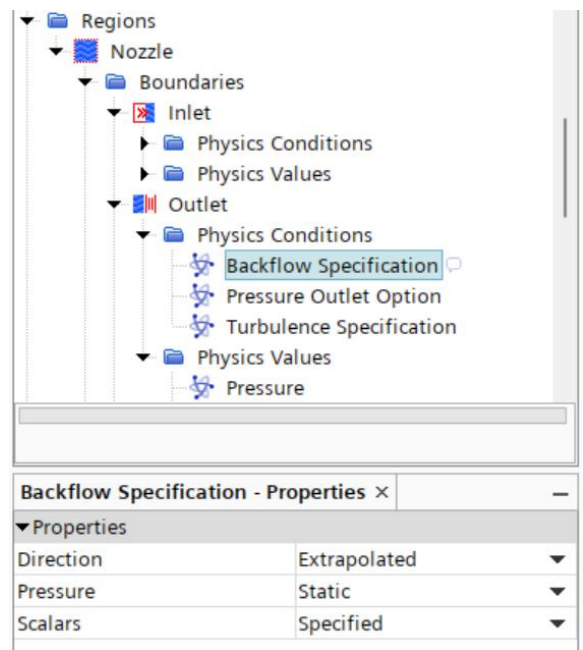
Note 6: this static parameter in step 106 tells the solution that the outlet will be evaluated based on the static pressure input. This is used due to the nozzle being in an enclosed system (wind tunnel). The environmental pressure is not present in this case, the outlet is presumably connected to another section.

p. Scenes

112.   To view the geometry and simulations right click on "Scenes"

113.   Select "New Scene"

114.   Select "Geometry", "Mesh", or "Scalar"
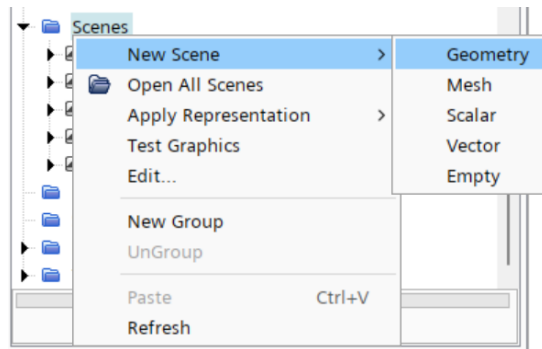
- The following images are the geometry, mesh, and scalar scenes

<Select Function>
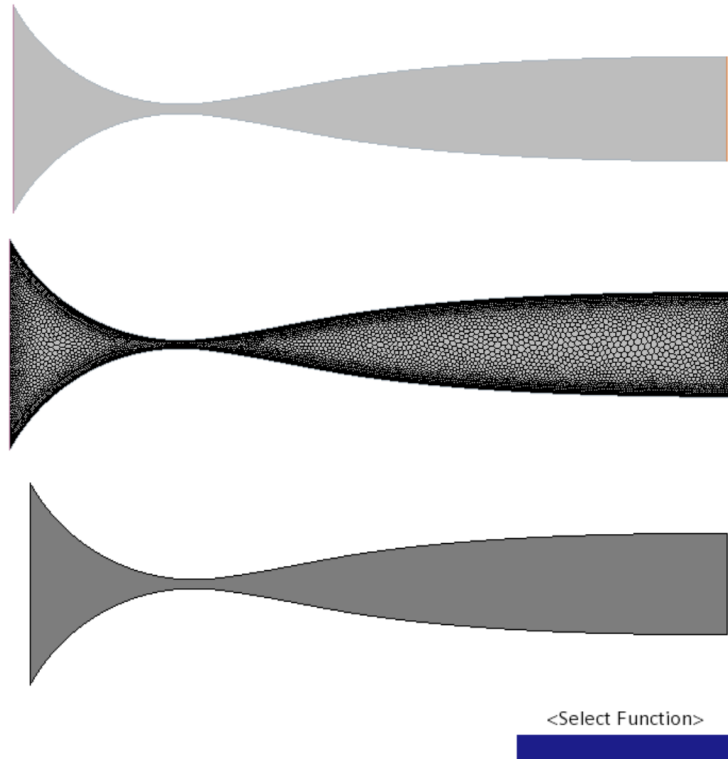
115.   Select "Scene/Plot" tab located on top of the simulation tree

116.   Expand "Scalar 1"

117.   Select "Scalar Field"

118.   Pick a function
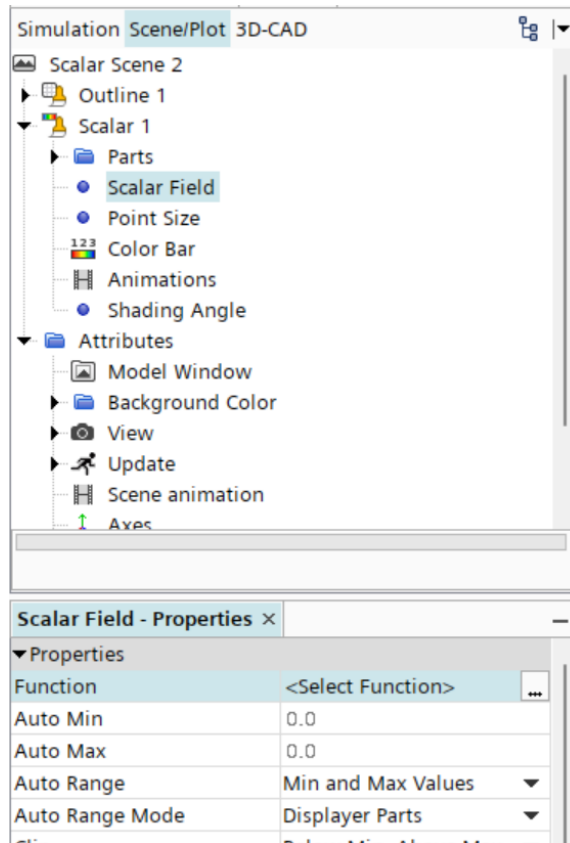
119. To view the Mach number profile type "Mach" in the search bar.

120. Expand "Mach Number"

121. Select "Lab Reference Frame"

122. Click "OK"
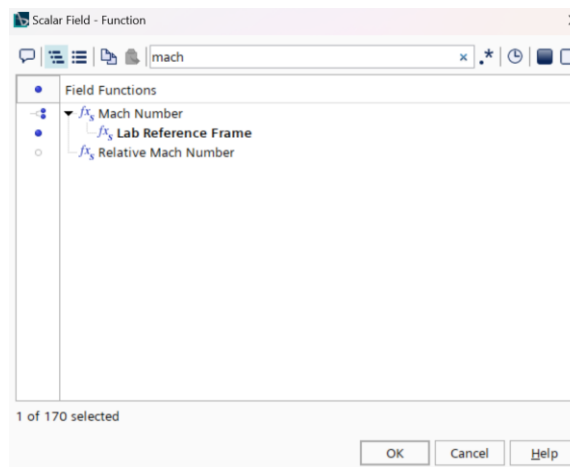
q. Run Simulation

123.   Click on the running stick man icon
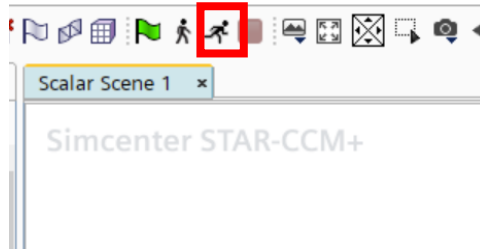
Enchance Scene Visual
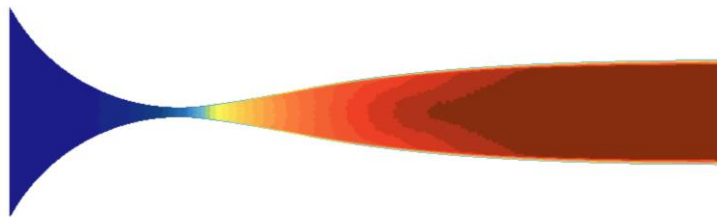
The mesh geometry distors the visualization of the scalar profile. To smooth it

out:

124.   Select "Scalar 1"

125.   Change "Contour Style" to "Smooth Filled"
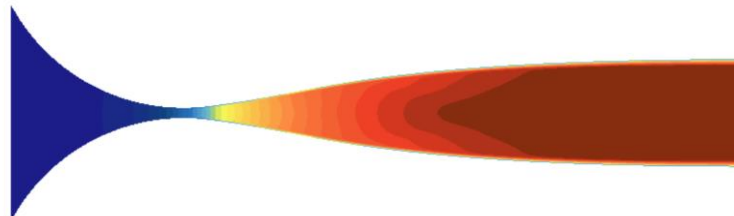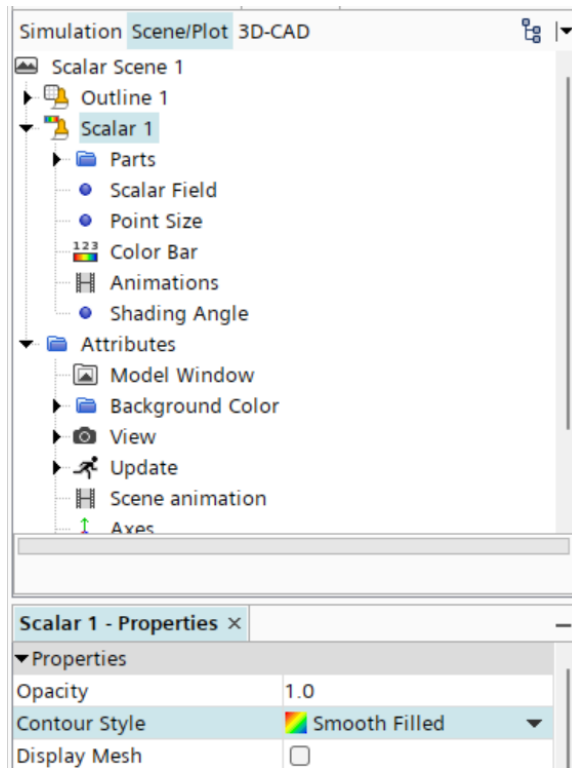
r. Iterations

126.   If more iterations are required. Expand "Stoping Criteria" section

127.   Select "Maximum Steps"

128.   Input desired amount in "Maximum Steps"
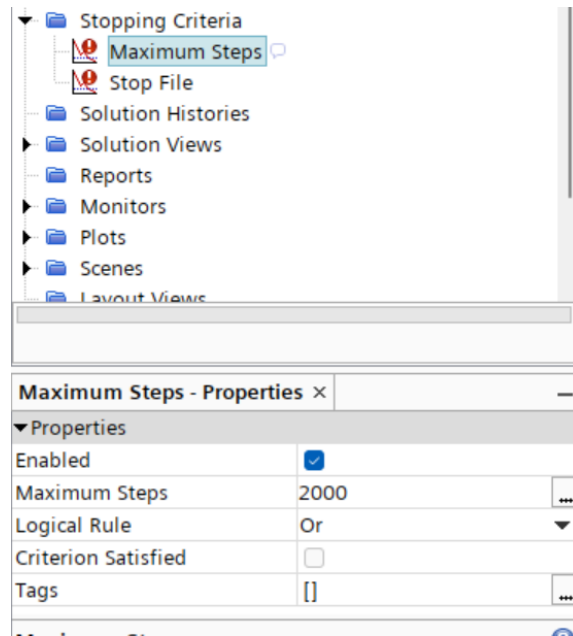
129.	Continue running simulation

TRANSIENT COMPREHENSIVE SIMULATION SETUP

Transient simulations require a set of different configurations but most of the models remain the same. The steady state solution can be copied but the following parameters must be changed:

s. **Transient Physics Continua**

130.	Expand "Continua" section

131.	Right click on "Models"

132.	Click on "Select Models"
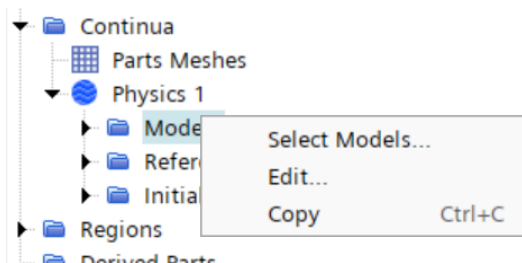
133. For time select "Implicit Unsteady". Everything else stays the same as for steady state.
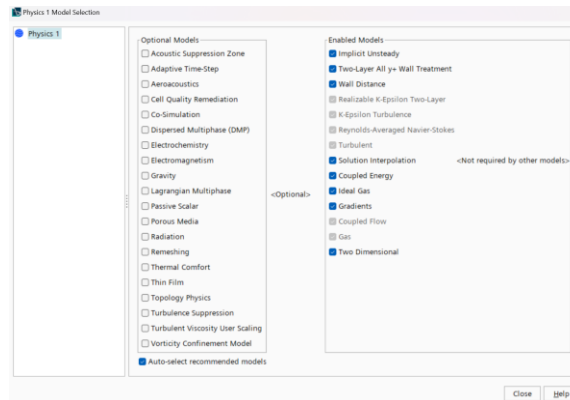
t. **Transient Solver**

134. Expand "Solver" section

135. Select "Coupled Implicit" section

136. For "Explicit Relaxation Method" set it to "Constant"
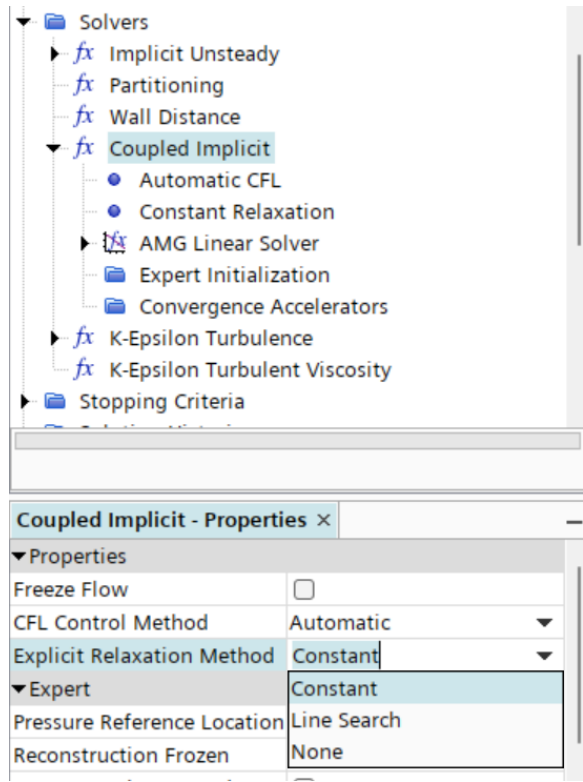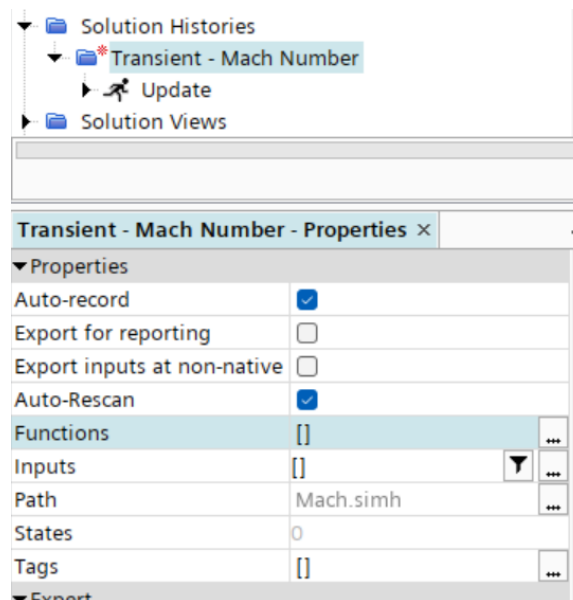
Note 7: *The CFL method must be changed to Automatic. The same values from steady state were used.*
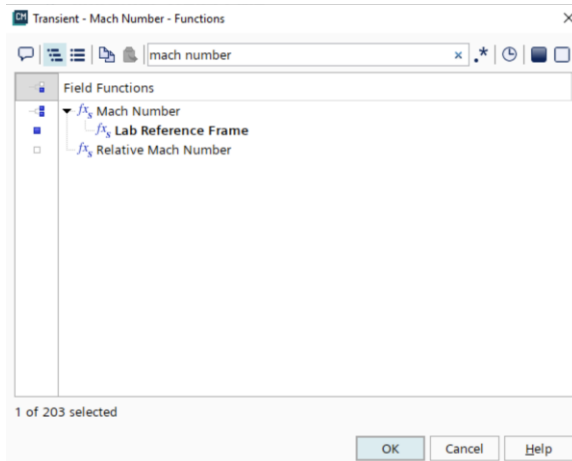
u. Record Transient Simulation

137.   Right click on "Solution Histories"

138.   Click on "New"
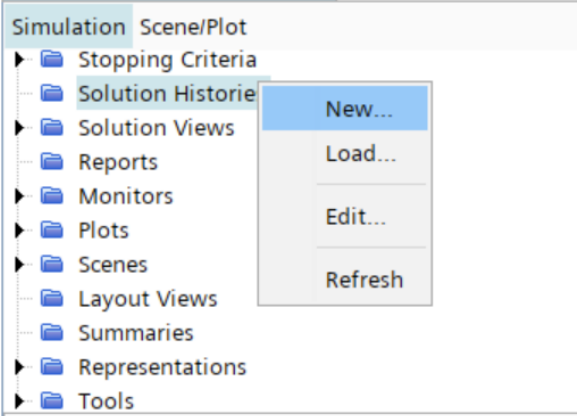
139. Name the file "Transient - Mach Number"

140. Save

141. Select "Transient - Mach Number"

142. Select "Functions"
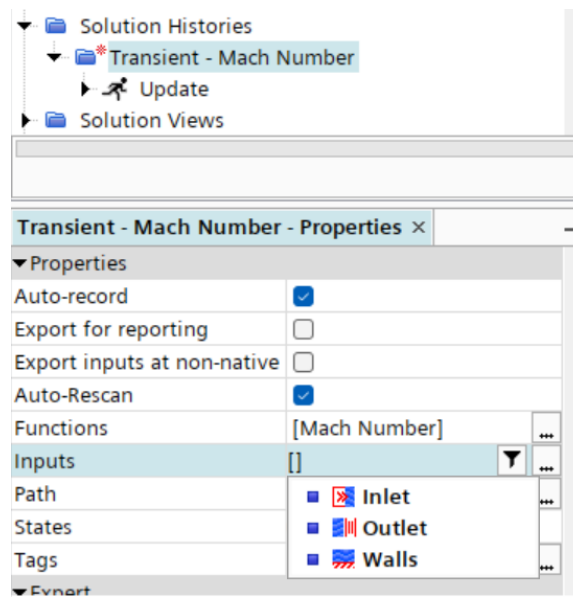

143. Search "Mach"

144. Expand "Mach Number" section
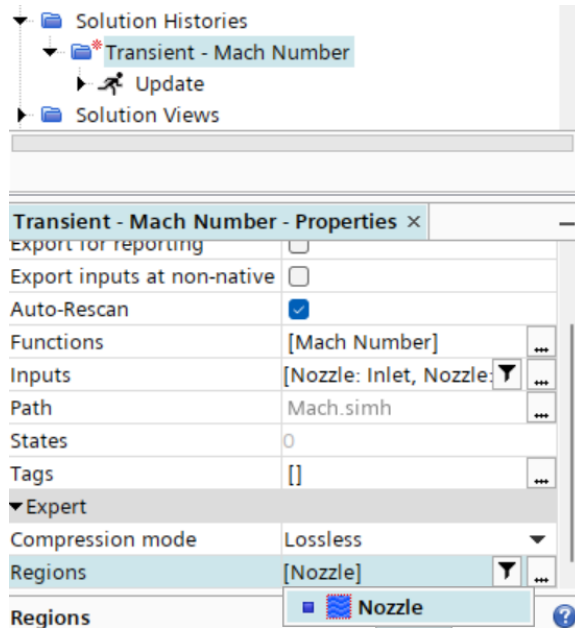
145. Select "Lab Reference Frame"

146. Click "OK"

147. Click on "Inputs"

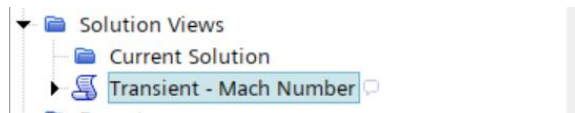148. Select "Inlet", "Outlet", and Walls

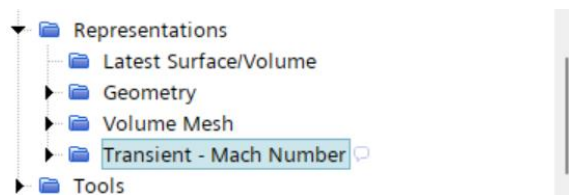149. Click on "Regions"

150. Select "Nozzle"

151. Expand "Solution Views" section

152. Left click, hold, and slide "Transient - Mach Number" tab onto Mach Number Scene
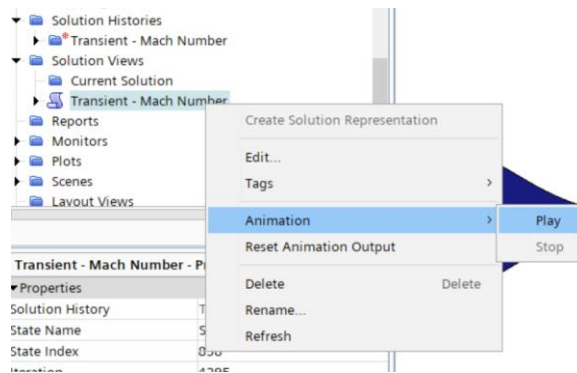

153. Expand "Representations" section

154. Left click, hold, and slide "Transient - Mach Number" tab onto Mach Number Scene

155. Run simulation and wait for it to fully converge or finish

165. Right click on "Transient - Mach Number" solution view

166. Select "Animation"

167. Click "Play" (transient video will play automatically)

Vita

Omar Antonio Dominguez obtained his bachelor's degree in mechanical engineering at the University of Texas at El Paso (UTEP) and further continued his education towards a master's degree in mechanical engineering conducting research at the Aerospace Center by developing his project emphasized in hypersonic applications by implementing High-Speed Wind Tunnel practices which led him to write his thesis. His experience led him to pursue a career with Sierra lobo Inc. as a propulsion engineer and later obtain the opportunity to be part of the National Nuclear Security Administration (NNSA) graduate fellowship program with the Pacific Northwest National Laboratory (PNNL) class of 2024.

Contact Information: theomaradt@gmail.com